Multi-Timescale Dynamics of Land Surface Temperature

A thesis

Presented to

The College of Graduate and Professional Studies

Department of Earth and Environmental Systems

Indiana State University

Terre Haute, Indiana

In Partial Fulfillment

of the Requirements for the Degree

Master of Art

---

by

Peng Fu

06/2014

Keywords: Multi-timescale, LST, trend, seasonality, decomposition, urbanization

COMMITTEE MEMBERS

Committee Chair: Qihao Weng, Ph.D

Professor

Department of Earth and Environmental Systems

Committee Member: Jennifer Latimer, Ph.D

Associate Professor

Department of Earth and Environmental Systems

Committee Member: Stephen Aldrich, Ph.D

Assistant Professor

Department of Earth and Environmental Systems

ABSTRACT

Spatial and temporal patterns of land surface temperature (LST) have been used in studies of surface energy balance, landscape thermal patterns and water management. An effective way to investigate the landscape thermal dynamics is to utilize the Landsat legacy and consistent records of the thermal state of earth's surface since 1982. However, only a small proportion of studies emphasize the importance of historical Landsat TIR data for investigating the relationship between the urbanization process and surface thermal properties. This occurred due to the lack of standardized LST product from Landsat and the unevenly distributed remote sensing datasets caused by poor atmospheric effects and/or clouds. Despite the characterization of annual temperature cycles using remote sensing data in previous studies, yet the statistical evidence to confirm the existence of the annual temperature cycle is still lacking. The objectives of the research are to provide statistical evidence for the existence of the annual temperature cycle and to develop decomposition technique to explore the impact of urbanization on surface thermal property changes. The study area is located in Los Angeles County, the corresponding remotely sensed TIR data from Landsat TM over a decadal year (2000-2010) was selected, and eventually a series of 82 cloud-free images were acquired for the computation of LST. The hypothesis technique, Lomb-Scargle periodogram analysis was proposed to confirm whether decadal years's LSTs showed the annual temperature cycle. Furthermore, the simulated LSTs comprised of seasonality, trend, and noise components are generated to test the robustness of the decomposition scheme. The periodogram analysis revealed that the annual temperature cycle was confirmed statistically with p-value less than 0.01 and the identified periodic time at 362 days.

The sensitivity analysis based on the simulated LSTs suggested that the decomposition technique was very robustness and able to retrieve the seasonality and trend components with errors up to 0.6 K. The application of the decomposition technique into the real 82 remote sensing data decomposed the original LSTs into seasonality, trend, and noise components. Estimated seasonality component by land cover showed an agreement with previous studies in Weng & Fu (2014). The derived trend component revealed that the impact of urbanization on land surface temperature ranged from 0.2 K to 0.8 K based on the comparison between urban and non-urban land covers. Further applications of the proposed Lomb-Scargle technique and the developed decomposition technique can also be directed to data from other satellite sensors.

PREFACE

This thesis is an original and unpublished intellectual product and an independent work by the author, P. Fu.

ACKNOWLEDGMENTS

First, I would like to express my deepest gratitude to my advisor Dr. Qihao Weng for his patient guidance and continuing support to conduct this thesis research. In August 2012 when I came to Indiana State University, Dr. Weng gave me one thesis book completed by a former master graduate student and told me directly that I need to write a thesis with pages at least the same as the sample he gave to me for graduation. I was shocked at the first time and during the following two years I tried my best in the research. Without his motivation, enthusiasm, and immense knowledge, this thesis could not have been accomplished successfully.

My sincere thanks also go to the rest of my thesis committee: Dr. Jennifer Latimer and Dr. Stephen Aldrich, for their encouragement, insightful comments, and hard questions.

Support from my parents and little brother is also an integral part for the completion of the thesis research. Thanks for their understandings for my absence when I should have stayed with them to celebrate every moment. Finally I am indebted to my fiancée for her love and support.

TABLE OF CONTENTS

COMMITTEE MEMBERS ii
ABSTRACT iii
PREFACE v
ACKNOWLEDGMENTS vi
LIST OF TABLES ix
LIST OF FIGURES x
CHAPTER 1 1
INTRODUCTION 1
1.1 Research background 1
1.2 Research Problem 2
1.3 Research Objectives 4
1.4 Structure of thesis 6
CHAPTER 2 8
LITERATURE REVIEW 8
2.1 Land surface temperature estimation 8
2.2 Urban Landscape Thermal Patterns 13
2.3 Urban heat island (UHI) intensity 15
2.4 Time-series LST data analysis 17
CHAPTER 3 21
STUDY AREA & DATA 21
3.1 Study Area 21
3.2 Data Sources 23
CHAPTER 4 25
METHODOLOGY 25
4.1 Statistical hypothesis testing for periodicity using Lomb–Scargle periodogram 26
4.2 LST decomposition 28

CHAPTER 5 31
RESULTS ANALYSIS 31
5.1 Rhythmic patterns analysis 31
5.2 Decomposition analysis 36
5.2.1 Test of the decomposition technique by simulated LST data 36
5.2.2 Application of the decomposition technique to remote sensing data 37
CHAPTER 6 42
DICUSSIONS & FUTURE WORK 42
CHAPTER 7 46
CONCLUSIONS 46
References 48

LIST OF TABLES

Table 5- 1 The tolerance of the Lomb-Scargle technique to data missing 34

Table 5- 2 Parameter values for simulating LST time series..... 37

LIST OF FIGURES

Figure 3- 1 The geographical location of study area 22
Figure 3- 2 The number of the image scene collected grouped by month..... 24

Figure 4- 1 Specific procedures for proposed study. 25

Figure 5- 1 The LST observations (A) and the corresponding Periodogram results including the power density (B) and the False Discovery Rate (C). 32

Figure 5- 2 The percent variance map explained by the identified annual temperature cycle over 2000-2010 34

Figure 5- 3 The sensitivity analysis of the decomposition technique by using simulated LSTs (Amplitude = 15, Trend = 0.1/per year). The preserved number of points represented the number of points used in the decomposition process. The absolute error was used to measure the errors in estimated trend component compared to the simulated trend..... 37

Figure 5- 4 Application of the decomposition technique to individual land covers including water, developed, barren, forest, shrubland, herbaceous, planted/cultivated, and wetlands. In each panel, the figure showed the original median LST observations, decomposed seasonality, trend, and noise components..... 40

CHAPTER 1

INTRODUCTION

1.1 Research background

Land surface temperature (LST), routinely mapped from remotely sensed thermal infrared (TIR) data to represent the skin temperature of the Earth's surface, is an indispensable parameter in analyzing and characterizing landscape thermal behaviors (Bechtel 2012), modeling surface energy balance (Oke *et al.* 1992, Friedl 2002, Renzullo *et al.* 2008), quantifying evapotranspiration for water management (Anderson *et al.* 2011, Anderson *et al.* 2012), and understanding the interactions between human activities and environmental change. Understanding of landscape thermal behaviors has displayed its profound implications in many fields including ecology (Luck & Wu 2002, Buyantuyev & Wu 2010), urban planning (Svensson & Eliasson 2002), hydrological cycles, and environmental pollution (Sarrat *et al.* 2006). Exploration of landscape thermal characteristics is usually dependent on the surface temperature parameter derived from the remotely sensed thermal infrared information.

The spatial and temporal distributions of landscape thermal patterns have implications for land surface processes and in turn, these processes have their alterations in LSTs. Urban areas are centers to a large proportion of the world's population, economic activities, and physical infrastructure that are subject to the impacts and risks of increased temperature, extreme heat

events, and heat islands (Romero-Lankao *et al.* 2012). Accordingly, detailed information of LST fluctuations contributes to the studies on urban vulnerability pertaining to the risks of temperature related hazards and may suggest the potential adaption strategy that can be adopted. Furthermore, it is also reported in the literature that surface temperature conditions are associated to the outbreak and propagation of vector-borne disease (Reisen *et al.* 2004, Ruiz *et al.* 2010, Liu & Weng 2012), and thus related to the quality of life. Therefore, estimation of LST and its distributions can not only facilitate the understanding of environmental and ecological processes, but also favor the concern of human well-being.

1.2 Research Problem

Rhythmic patterns occur at all land surface processes dominated by the annual cycle caused by the changes in solar radiation. Surface temperature is not an exceptional parameter controlled by the solar radiation fluctuations. Previous studies mainly focus on LST dynamics of the annual cycle, usually referred as $A(t)Cos(2\pi t+\theta)$, which can be attributed to the fact that surface temperature seasonality is incumbent, within a phase lag, on the yearly cycle of insolation at the top of atmosphere aroused by the Earth's changing position (Thomson 1995). However, it should be noted that solar radiation reaching land surface is not or no longer the same as that reaching the top of atmosphere due to the nonlinear response of earth climate and environmental system (Qian *et al.* 2011). This situation is further complicated by the increasingly rapid urbanization processes, characterized by the increase in sensible heat fluxes, decrease in latent heat fluxes, and an extra component of anthropogenic heat discharge in light of surface energy balance in urban areas (Oke *et al.* 1992, Zhou *et al.* 2012). The notorious

phenomenon, urban heat island (UHI), is a typical consequence resulting from the urbanization process. In turn, turbid spatial and temporal thermal patterns further disorder the urbanization rate, urban form, energy consumption and infrastructure configuration. These bidirectional feedbacks and interactions between urbanization and environmental change have received less attention compared to the myriad literature on whether and how urbanization has a positive or negative effect on the environment (Seto 2011).

The Landsat legacy and consistent records of the thermal state of earth's surface since 1982 represents hitherto the only long term archival TIR information with spatial scales appropriate for human scale studies globally (Schott *et al.* 2012). The time series Landsat image data provide a history of how urbanized land cover and ecosystem have evolved over the past 30 years in the face of increased human population, resource consumption, and environmental change. So far, only a small proportion of studies emphasize the importance of historical Landsat TIR data for investigating the subtle and dedicated inter-relationship between the urbanization process and climate variables. Possible reasons for underutilization of the Landsat archive may be imputed to the following aspects: 1) Although the open access data policy allows the procurement of Landsat data held by the United States Geological Survey (USGS) freely available (Wulder *et al.* 2008), an effort to completely and consistently calibrate the archive into absolute surface leaving radiance and to surface radiometric temperature is still in progress (Schott *et al.* 2012). Lack of atmospherically compensated and calibrated Landsat thermal radiance/LST operational products, unlike the MODIS operational thermal radiance and LST products, constrains the use of Landsat archive for characterizing landscape thermal patterns over a long time scale. 2) Technically, there exist difficulties in analyzing the alleged time series Landsat TIR data. The sampling frequency taken by the satellite sensor is fixed (e.g., 16 days for

Landsat), while the recorded information may be irregularly distributed because of constant cloud contamination and other poor atmospheric conditions (Ju & Roy 2008). These irregularly spaced data pose a challenge for extracting periodic patterns with known and acceptable confidence level using traditional statistics and techniques.

A popular computational technique utilized to identify rhythmic patterns is Fast Fourier Transform (FFT) (Priestley 1982), which isolates periodicities by searching for sharp peaks in the ordinary periodograms calculated from the Fourier transform of the time series. Van De Kerchove *et al.* (2013) differentiated the short term weather components from strong, climate related, periodic patterns by applying the FFT technique to the 8 year of MODIS both daytime and nighttime LST time series to unfold the complicities of spatio-temporal variations in the Russian Altay Mountains. An alternative way similar to FFT is to use a parametric model with fixed angular frequency, amplitude, and constant trend to fit the time series data. This method can be regarded as a derivative from FFT but differs itself from the decomposition into fixed and known frequency cycles. Bechtel (2012) proposed an annual temperature cycle (ATC) to characterize landscape thermal patterns and the sinusoidal model used to describe ATC is in the aforementioned style. Considering the global environment change as well as the urban local environment change, merely characterizing the long term ATC ignores the modifications caused by human disturbances, land management, and inter-annual climate change. Furthermore, it is at least worth discussion that land cover change and conversion by urbanization may cause changes in LST phonological cycle, i.e., changes in amplitude, angular frequency, and trend. Therefore, new ways are still needed to develop for exploring the LST variations.

1.3 Research Objectives

In general, it is assumed that there should be four types of changes within LSTs: 1) seasonal dynamics (phenology cycle), driven by the changes in surface solar insolation; 2) gradual changes such as the inter-annual climate variability or gradual change caused by land management or land degradation; 3) abrupt changes, caused by urbanization, fire, or deforestation; 4) inconsequential changes caused by the short-term weather conditions, such as rainfall and clouds. A challenge in examining the relationship between urbanization and environmental change is how to isolate the thermal fluctuations attributed to urban activities amidst background variations. In addition, it should be noted that urbanization related activities can also result in alterations in these three types of changes. Analyses in Weng &Fu (2014) presented that LST seasonal dynamics differed in each land cover and suggested possibly disordered thermal variations in urban areas. Since urban expansion means the replacement of natural settings by impervious surface, there will be corresponding modifications in LST phenology cycle. The existence of urban micro-climate, such as UHI and urban canyon phenomena, can also lead to abrupt changes. Thus, a question of interest is: Over what time-scale are urbanization related activities coupled with LST dynamics?

Based on the aforementioned challenges, specific objectives of this research include: 1) to provide the statistical probability evidence for the existence of periodic patterns within LSTs; 2) to propose new methods to decompose unevenly spaced LST time series into a seasonal, a trend and a stochastic component; 3) to validate the efficiency of proposed method by using both simulated LST data and the Landsat time series data; and 4) to analyze the impacts or changes imputed to urbanization activities in the decomposed components. The hypothesis to be tested is that urbanization processes/human activities weaken land surface temperature annual cycles, i.e.,

there is a weakened seasonality in urban areas compared to rural locations. Aside from this speculation, it is conjectured that there are much more strongly intensified inter-annual trend variations in conurbation areas than those in the surrounding sylvan regions. Specifically, it is predicated that urbanization related activities intensify the inter-annual trend fluctuations besides the already known global warming trends. The statistical probability tests anticipate that differences exist in the variances explained in the different regions by the annual temperature dynamics. These hypothetical expectations all point to the same questions: How does urbanization affect LSTs and to what degree these LSTs are influenced by human activities?

1.4 Structure of thesis

The thesis is organized in six chapters. Chapter 1 “INTRODUCTION” focuses on the introduction to the research, including research background, research problem, research objective, and thesis structure. Chapter 2 “LITERATURE REVIEW” places efforts in reviewing significant publications in land surface temperature mapping, urban landscape thermal patterns from an ecological perspective, and the current state-of-art methods in analyzing time series LST data. The land surface temperature mapping not only summarizes the direct ways to derive LST maps from the Landsat thermal sensors, but also outlines the potential techniques used to downscale coarse TIR data from other sensors (e.g., MODIS, GOES) to the fine Landsat spatial resolution. Both temporal and spatial enhancements of the TIR data are presented. Currently, there is a lack of detailed review in urban thermal landscape patterns, especially from an urban ecological perspective. The review here attempts to provide some insights into the current urban ecology studies. Furthermore, the time series LST data analysis section discusses the current techniques

employed to analyze long term remotely sensed data. Chapter 3 and Chapter 4 detail the proposed study area, data procurement and processing, and methodology, respectively. Chapter 5 presents the results analysis based on which, Chapter 6 transfers and discloses the conclusions and discussions. Potential applications, as well as the limitations of proposed research will also be discussed in details in this section.

CHAPTER 2

LITERATURE REVIEW

This chapter reviews the methods used for mapping LST, studies pertaining to landscape thermal patterns, and techniques used for dealing with time series data. The last part of the review aims to support the worth of the proposed study to utilize the long term-series stack for analyzing urban environmental change.

2.1 Land surface temperature estimation

Surface temperature estimation based on satellite sensors ranges from spatial scales of dozens of meters (e.g., Landsat TM/ETM+) to several kilometers (e.g., GOES, SEVIRI). Different methods have been developed for mapping surface temperature by compensating the brightness temperature, i.e., converted by using the top of atmosphere radiance, for the atmospheric absorption effects to estimate the surface leaving radiance. Since the focus of the study centers on the utilization of Landsat TM for analyzing the human related thermal patterns, the review of LST mapping here only lists the technique devised specifically for Landsat sensors.

Remotely sensed thermal infrared information proves to be an efficient facility to deliver LST maps at varying scales and over years, a substantial number of techniques and algorithms

have been devised for achieving this goal, including split-window, two/multi-channel algorithms, and two/multi-angle methods (Sobrino *et al.* 1996, Sobrino *et al.* 2004, Dash *et al.* 2005). Landsat sensors (until Landsat 7) consist of six bands with one thermal bands in the range from 10.4μm to 12.5μm. Basically, there are three different methods for retrieving LST from Landsat TM/ETM+ thermal infrared sensors (Sobrino *et al.* 2004) and these techniques share a common physically theoretical basis which can be described by the radiative transfer equation (RTE) (Ottle & Stoll 1993).

$$L_{sensor,\lambda} = \left[\varepsilon_\lambda B_\lambda(T_s) + (1-\varepsilon_\lambda)L^{\downarrow}_{atm,\lambda}\right]\tau_\lambda + L^{\uparrow}_{atm,\lambda} \ldots\ldots\ldots\ldots\ldots\ldots\ldots (1)$$

Where $L_{sensor,\lambda}$ is the at-sensor radiance or Top of Atmosphere (TOA) radiance, i.e., the radiance measured by the sensor. ε_λ is the land surface emissivity, $B(T_s)$ is the blackbody radiance given by the Planck's law and T_s is the LST. $L^{\downarrow}_{atm}$ is the down-welling atmospheric radiance, τ is the total atmospheric transmissivity between the surface and the sensor, and $L^{\uparrow}_{atm}$ is the upwelling atmospheric radiance. The variants of the deriving methods for LST estimation depend on how to obtain the necessary parameters to solve the radiative transfer equation.

The direct utilization of RTE relies on the in situ atmospheric radiosoundings which are generally input into a radiative transfer code, such as MODTRAN (Berk *et al.* 1987) to simulate the parameters of atmospheric transmissivity, up-welling and down-welling radiances. Then the surface leaving thermal radiances can be calibrated and compensated for the atmospheric effects through the RTE and thus converted to surface temperature with known land surface emissivity values. It should be noted that the RTE depends on the wavelength considered, bandwidth, view angle and spectral response function. This method is the most straightforward way to derive LST whereas the limitation remains in the situation where, in most cases, lack of such in situ data at the same with the satellite overpass time is routine.

In order to avoid the dependence on the in situ radiosounding data, Qin *et al.* (2001) developed a mono-window algorithm for acquiring LST for TM sensor. By simplifying the Planck's law into a linear expression, the proposed algorithm eventually transformed the RTE equation to an expression integrated by the brightness temperature and atmospheric mean temperature. Although it does not require as many atmospheric profiles as the direct utilization of RTE, near surface air temperate and water vapor properties are also needed for estimating the mean atmospheric temperature and transmissivity. Qin's technique is relatively easy to implement, despite its unclear definition of atmospheric mean temperature and its constraints of using meteorological data.

Finally, Jimenez-Munoz &Sobrino (2003) proposed a generalized single channel algorithm for retrieving LST driven by the total atmospheric water vapor content. The dependence on water vapor content is due to the fact that this atmospheric content is the main absorber in the thermal infrared region. The atmospheric function used in the algorithm was simulated using the MODTRAN codes with inputs from the TOVS Initial Guess Retrieval (TIGR) database for each specific sensor. In spite of a general spectral response function, Gaussian filter, used in the study for the effective wavelength estimation, a particularized one was also computed for Landsat sensors. Compared to the two techniques mentioned above, the main advantage of the generalized single channel algorithm is that in situ radiosoundings or effective atmospheric mean temperature values are not required in addition to the convenient extension of the method to other thermal sensors.

All these methods require the inputs of land surface emissivity values into the RTE for inverting LSTs. The effects of land surface emissivity on satellite measurements can be categorized into the following aspects including the reduction of surface emitted radiance and the

uncertain variations (i.e., either increase or decrease) in radiance caused by the anisotropy (Prata 1993). Accurate emissivity values are, therefore, essential for recovering thermal radiances from multi-spectral images. Emissivity is a function of wavelength, while at the meantime, it is controlled by such factors as surface roughness, structure, soil moisture content, chemical composition (Snyder *et al.* 1998). Emissivity estimation for surface features from the remotely sensed data has been computed using different techniques, including the normalized emissivity method (Gillespie 1986), thermal spectral indices (Becker *et al.* 1992), spectral ratio method (Watson 1992), Classification based method (Snyder *et al.* 1998), and the temperature-emissivity separation (TES) method (Gillespie *et al.* 1998), and the NDVI-threshold method (Sobrino *et al.* 2008). Depending on the study properties, these methods can be selected for estimating surface emissivity values prior to recovering LSTs except the TES method, which requires at least two thermal channels for calculation.

Other than the mapping methods aforementioned, efforts have also been made to enhance the thermal infrared information of coarse resolution to approximate Landsat spatial scale (~100 m), referred as *downscaling*, *disaggregation*, or *thermal sharpening*. Algorithms dedicated to the spatial or/and temporal enhancement of LST images can fall into two broad categories: (1) the statistical based methods and (2) the physical based models. The basic idea of the statistical method to achieve the downscaling scheme is to establish a reasonably functional relationship between TIR radiance/ LST and biophysical and/or socio-economic variables that are associated with LST variations. The assumption is the established function holds across different scales and the biophysical, socio-economical and other associated ancillary data can be easily acquired and scaled. The classic sharpening technique, known as TsHARP, enhances the thermal data using the inverse relationship between LST and Normalized Difference Vegetation Index (NDVI)

(Kustas *et al.* 2003). However, studies have showed that the LST-NDVI relationship is ill defined over many complex heterogeneous landscapes (Inamdar & French 2009, Merlin *et al.* 2010, Dominguez *et al.* 2011, Jeganathan *et al.* 2011) and thus the approach could be applied locally within relatively homogeneous sub-regions, but not on a regional basis.

The physical models are usually involved in utilizing the spectral mixture analysis (SMA) to achieve the downscaling purpose. It should be noted that the application of SMA into the spatial enhancement of thermal information has technical limitations, i.e., twice as many thermal bands as the number of end-members are required and rarely more than five appropriate bands are available (Zakšek & Oštir 2012). Therefore, studies using SMA decompose the TIR pixel into multiple isothermal components and produce a set of component temperature (Dozier 1981, Gillespie 1992, Liu & Pu 2008). However, this method has been accused of providing no solution on the position of each component (Liu & Pu 2008, Zakšek & Oštir 2012).

In spite of the progresses made by these downscaling techniques and algorithms, thermal sharpening techniques cannot replace the actual thermal imagery at fine resolutions or missions that provide high quality thermal band imagery at high temporal and spatial resolution critical for many land and water resource management applications (Gao *et al.* 2012). Compared to a large proportion of literature on downscaling development, less attention has been paid to the direct computation of LST from Landsat sensors. This is evident considering the unavailability of operational LST product from Landsat achieve. To some extent, the lack of consistent and accurate LST maps constrains the further extraction of valuable information from historical records. As a result, effective methods for generating operational LST maps are highly demanded and sought.

2.2 Urban Landscape Thermal Patterns

Urban landscape thermal patterns originate from landscape patterns studied in the field of landscape ecology to explore the causes and consequences of spatial heterogeneity across a range of scales (Turner *et al.* 2001). Most studies pertaining to the landscape thermal patterns focus on the relationship between landscape patterns and LST variations in the urban areas. A typical topic of landscape thermal patterns is to examine impacts of land cover and land use configuration and composition on LST variations.

Weng *et al.* (2004) investigated the interplay between thermal and vegetation dynamics by using vegetation fraction derived from the linear spectral mixture analysis (LSMA). The analyses suggested that the areal measure of vegetation abundance by unmixed vegetation fraction possessed a more direct correlation with the radiance, thermal, and moisture properties of Earth surface that determined LST. Yuan &Bauer (2007) presented that the relationship between percent impervious surface and LST was much stronger than that between NDVI and LST in urban areas. Xian &Crane (2006) conducted a research by using the sub-pixel impervious surface and land use data to identify surface thermal characteristics and patterns. Detailed examination demonstrated that thermal effects are strongly correlated with urban development densities in which the higher temperature is usually associated with higher imperviousness surface. Lu &Weng (2004) developed a spectral mixture analysis to explore the relationship between urban thermal features and landscape pattern types in the City of Indianapolis, Indiana. The results suggested that impervious surface and LSTs had a positive linear relationship while vegetation and LSTs had a negative linear relationship for the study area. Small (2006) presented a comparative analysis of urban reflectance and surface temperature for

24 urban areas and their surrounding areas using Landsat ETM+ imagery. The researcher discovered that the urban thermal fields varied across regions and identified a visible variability in the inverse correlation between surface temperature and vegetation fraction at moderate spatial resolutions. Chen *et al.* (2006) explored the relationship between urban heat island and land use/cover. By utilizing several biophysical indices, the presented study employed a regression analysis and found out that the spatial distribution of urban heat island has been changed from a mixed pattern to an extensive one, in which higher LSTs scattered across the land cover. They also discovered a negative relationship between NDVI, NDWI and temperature, while a positive relationship between NDBI and temperature. Deng &Wu (2013) proposed a two-step physically based method, spectral unmixing and thermal mixing (SUTM) to investigate the impacts of urban composition on landscape thermal patterns. The evidence that the SUTM outperformed other regression analyses for NDVI, percent impervious area, and percent vegetation may imply the complicated function of land cover composition on surface temperature distributions.

In addition to the directly quantitative analysis to assess the interplay between land cover abundance and thermal characteristics, landscape metrics are also utilized to discuss how landscape dynamics affect LST variations or how landscape patterns of LST are influenced by the land cover configuration. The integration of landscape metrics and remote sensing allows correlating the surface characteristics with LST variations in evaluating the thermal behaviors and dynamics of landscapes (Weng *et al.* 2007). Li *et al.* (2011) found a strong correlation between the mean LST and landscape metrics, indicating that the urban landscape configuration also influences the formation of urban heat island by employing ETM+ images. Weng *et al.* (2007) assessed the effects of land use and land cover patterns on thermal conditions using landscape metrics at landscape land cover level. The derived LST maps were also divided into

each zone based on mean and standard deviation values so as to quantify the thermal dynamics. The use of landscape metrics allows the comparisons between land cover composition and thermal patterns. These findings are helpful for understanding urban ecology as well as land use planning to minimize the potential environmental impacts of urbanization. Nonetheless, as the same in the landscape ecology, the scale issues should be dealt with carefully due to the increased LST and land cover heterogeneity. Liu & Weng (2009) conducted a scale analysis in terms of the relationship between landscape patterns and LST. The case study in Indianapolis concluded that thirty meter was the optimal spatial resolution in the study of the relationship between urban LULC and LST classes and that ninety meter was the optimal resolution for assessing the landscape-level relationship between LULC and LST patterns.

However, these studies only focus on the impacts of landscape patterns on thermal variations, and ignore how different landscape configuration/composition brings about different alterations in the overall thermal characteristics. In other words, the presented studies only investigate the static relationship between landscape patterns and thermal behaviors. Detailed analyses into the dynamic changes into the landscape patterns are promising to shed some lights on the current dark aspects.

2.3 Urban heat island (UHI) intensity

One special aspect that evolves from the characterization of landscape thermal patterns, which is also one of the objectives to monitor thermal conditions, is to develop efficient and effective indicators and/or models to represent the intensity of urban heat island. The term urban heat island (UHI) states the phenomenon of altered temperatures in urban areas compared to their

rural regions (Oke 1982, Voogt & Oke 2003, Kim & Baik 2005) due to the replacement of natural land covers with impervious surfaces, such as parking lot and concrete highways. The UHI not only lowers the quality of life (Harlan *et al.* 2006, Lafortezza *et al.* 2009), but also alters the ecological functions, such as the provision of air quality and water resources (Grimm *et al.* 2008), and biodiversity (Knapp *et al.* 2010).

An important and critical issue in urban thermal remote sensing is how to quantify UHI observed at meso-scale and macro-scale by using pixel-based LST measurements (Weng *et al.* 2011). The most simple and direct, as well as the classic way to compute the UHI intensity is to compute the difference between urban and rural temperatures (Roth *et al.* 1989, Dousset & Gourmelon 2003). However, the definition of urban and rural is not consistent and confusing (Schwarz *et al.* 2011) in the remote sensing studies. Imhoff *et al.* (2010) defined urban ring zones based on the percent impervious surface area(ISA) while stated that the rural zones are pixels located in 5 km wide ring ranging between 45 km and 50 km away from the 25% ISA contour. The researchers unfolded that ecological context significantly influences the urban heat island intensity. Furthermore, the difference of pixels around urban and rural weather station (Tomlinson *et al.* 2012), and around the selected downtown and rural districts (Dousset & Gourmelon 2003) has also been used to quantify the intensity of UHI.

Other than the traditional *difference* means to measure the UHI magnitude, several other indicators have also been developed. Streutker (2003) utilized a least square fit of the entire heat island to a Gaussian surface from which the magnitude, spatial extent, orientation, and central location of the UHI can be determined. Based on a non-parametric model, Gaussian process, Rajasekar &Weng (2009) quantified the UHI magnitude, spatial pattern and intensity and illustrated how the landscape thermal patterns evolve over space and time using the MODIS time

series LST stacks. In a research conducted by Zhang &Wang (2008) to study the relation of spatial extent of UHI to urban characteristic factors, an indicator of hot island area (HIA) was proposed to quantify the evolvement of UHI. The HIA is defined as a region possessing LST values greater than the mean plus one standard deviation. The non-parametric model and the HIA representation are examples of the indicators that do not dictate the prior definition of urban and rural boundary.

Despite of the valuable progresses, a recent review presented by Schwarz *et al.* (2011) suggested that these indicators individually revealed diurnal and seasonal variations and show a relatively low correlation over time. Thus, it can be concluded that temporal aspects and selection of indicators are import factors determining the UHI intensity estimation (Schwarz *et al.* 2011). Cautions should be placed to the instabilities and inconsistence of these indicators and using some of these indicators in parallel may help describe the UHI properly.

2.4 Time-series LST data analysis

The utilization of remotely sensed time series stacks for extracting useful information for investigating landscape thermal dynamics have received less attention compared to a substantial number of literatures concentrating on employing only one or several images for analyses. These studies seem to suggest the dynamics appear to be “static” as if they do not change over time. In the earlier time, a critical issue faced by the scientific communities is the pressing demand for the procurement of thermal infrared data delivered by satellite sensors. However, current status has been shifted to how to utilize the large amount of thermal data, such as information from Landsat and MODIS (Weng & Fu 2014). The recent *Urban Observatory* project

(http://www.urbanobservatory.org/) initiated by the *ESRI Inc.* to showcase the remote sensing, census, and other derivative data for many global cities, which allows the comparisons among cities in different dimensions, may also represent an innovative way to use the large amount of data that currently the scientific communities have. The connotation transmitted by the observatory project is that it is worthy of extracting valuable information through the mass data for answering questions related to the impacts occurring in global cities. Moreover, the recent GEO work plan (the sub task-global observation and information 2012-2015) identifies objectives to support development of global observation and analysis system and to produce up-to-date information on the status and development of the urban system. Naturally, the assets of the existing remotely sensed archive should be an indispensable part of the to-be-established urban system, which will allow the real time monitoring and assessment of the built-up environment.

In spite of the fact that only a few studies have been conducted by utilizing the thermal time series stacks for urban remote sensing studies, useful data mining techniques have already been devised to reduce the data amount. Gottsche &Olesen (2001) employed a harmonic and an exponential term to model the diurnal cycles of surface temperature derived from the Geostationary Operational Environmental Satellite (GOES). The proposed diurnal characterization reduced the 48 measurements per pixel to 5 parameters, advantageous to the climatological studies which require the processing of long term time series. Keramitsoglou *et al.* (2011) used a total of 3401 MODIS LST images to reveal the magnitude, spatial extent, and maxima of thermal patterns in Greater Athens area, Greece by virtue of an object-based image analysis method. Although these studies are merely based on the coarse resolution thermal data, the data mining methods may also be suitable for high spatial resolution thermal data. Bechtel

(2012) discovered that modeling the annual temperature cycle (ATC) with Landsat archive was also feasible to obtain the mean annual surface temperature, yearly amplitude of surface temperature, and phase shift parameters. His study in the city of Hamburg, northern Germany, collected 35 thermal images from Landsat-5 and -7, and estimated approximate 1 K accuracy for the ATC model. Weng &Fu (2014) further analyzed the ATC model, correlated the derived parameters to surface biophysical descriptors, and suggested that the parameters can be acquired even at cloudy conditions. These efforts, to our knowledge, represent the current frontiers to take full advantage of time series data in thermal studies of remote sensing.

A detailed survey of how NDVI time series have been utilized for modeling ecosystem functions and dynamics can also shed lights for the current thermal remote sensing studies. A previous focus of the relevant projects is to recover clear-sky NDVI time series considering the frequent contamination of clouds and the atmospheric instability. Roerink *et al.* (2000) described the Harmonic ANalysis of Time Series (HANTS) algorithm to remove cloudy observations and interpolate the missing measurements for reconstructing gapless NDVI values. With the assumptions that NDVI time-series follow annual cycles of growth and decline of vegetation, Chen *et al.* (2004) proposed a simple but robust method to smooth out noise in NDVI time-series based on the Savitzky–Golay filter. Seasonal vegetation variations are closely associated with vegetation phenology, such as green-up, peak and offset of development (McCloy & Lucht 2004). Various algorithms and techniques use time series NDVI to derive parameters to describe the vegetation phenology and production that are of primary importance for modeling vegetation dynamics (Pettorelli *et al.* 2005). Methods for modeling NDVI time series include Fourier analysis (Juarez & Liu 2001, Wagenseil & Samimi 2006), wavelet decomposition (Martinez & Gilabert 2009), and curve fitting (Paruelo & Lauenroth 1998).

Despite the valuable techniques, these studies only have the capacity to quantify the vegetation phonological cycle while ignore the internal changes caused by the varying disturbances, such as deforestation, urbanization, and wildfire. Subject to the possible interruptions to the ecosystem, the developed methods may also show the inconsistence although they are assumed to quantify the same vegetation phenology. Recent studies presented by Verbesselt *et al.* (2010) suggested that decomposition of time series NDVI into different components made possible the real-time disturbance detection that contributed to investigation of seasonal, gradual, and abrupt changes. Therefore, establishing a standard analysis system based on the time series remotely sensed data would be useful for understanding ecosystem dynamics and functions.

Lessons can be learned from studies using NDVI time series for the landscape thermal variations. Current research projects in the thermal field to utilize time series stacks pay their primary attention in quantifying LST fluctuations over space and time. The coupling relationship between thermal variations and the environment have been relatively neglected. In the large scale, it is evident that there is a global warming taking place, while at the regional/local scale the urbanization is also influencing the environment. The implications brought by the interactions of the global and regional environment and climate change remain unresolved. Therefore, the future research should be directed to deepen the current understanding of specific thermal changes, how they interact with environment, and the current transition to sustainability.

CHAPTER 3

STUDY AREA & DATA

3.1 Study Area

The study area consists of nearly the whole Los Angeles County, California, except for the southern part and two offshore islands, the Santa Catalina Island and the San Clemente Island. According to the 2000 census, the county has a total area of 4752.32 square miles, of which 85.5% is land and the remaining is water. Los Angeles County is the most populous county in the nation, with a population of 9,818,605. The primary mountain ranges are Santa Monica Mountains and the San Gabriel Mountains in the southwestern and southeastern part of Los Angeles County, respectively. The Mojave Desert / barren land begins at the northeastern part of the county and stretches westward. The valleys are largely the population centers, and compose a large percentage of the urban areas. This area comprises of geographically diverse regions ranging from hilly mountains, deep valleys, ocean coastlines, forests, lakes, rivers, and barren land. The National Land Cover Database (NLCD) 2006 (available at http://www.mrlc.gov/nlcd06_data.php) identified 8 land cover types in the study area, i.e., water, developed, barren, forest, shrubland, herbaceous, planted/cultivated, and wetlands (Fig. 3-1). This geographical diversity made it an ideal study area for the examination of LST variability. Besides, the selection of the study area as

the Los Angeles County is due to its greater chance to acquire clear sky images than other regions, such as Chicago or Houston, to facilitate the subsequent time series analysis.

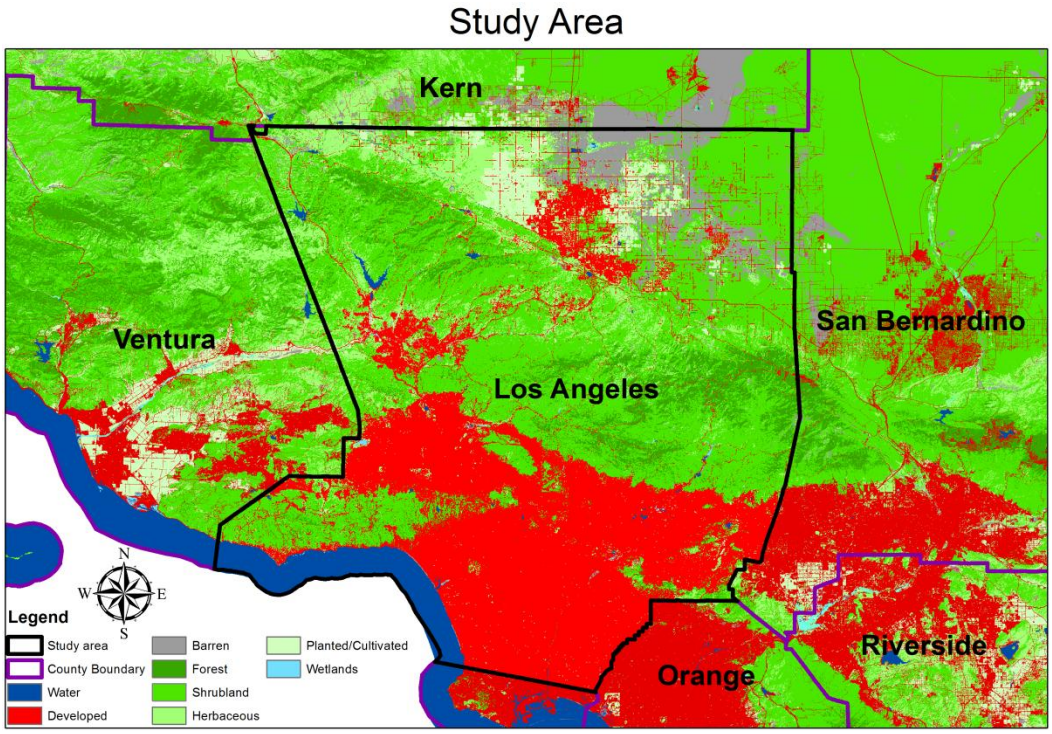

Figure 3- 1 The geographical location of study area

The area possesses a Subtropical-Mediterranean climate with a dry summers and moist winters. The average high air temperature is 29 ˚C in August and 20 ˚C in January based on the weather records from the Downtown-University of Southern California campus. Temperature experiences apparent change between the inland and coastal areas, as elevation and the distance to the coast increase. According to a study by the urban heat island group, the urbanization of city has negatively affected the urban community, such as the increased energy use, impaired air quality, and the aggravation of heat-related and respiratory illness (http://heatisland.lbl.gov/coolscience/cool-science-urban-heat-island). Los Angeles has a known problem in air quality, which is related to its UHI phenomenon. According to the Heat Island

Group (http://heatisland.lbl.gov/), the heat island effect costs about US $100 million per year in energy.

3.2 Data Sources

An operational LST product from Landsat TM/ETM+ archive will definitely benefit the current research. Considering that the product is still in progress, an alternative way to derive LST maps is to use the NASA Correction Parameter Calculator (Barsi *et al.* 2005), which uses the National Centers for Environmental Prediction (NCEP) modeled atmospheric global profiles interpolated to a particular date, time, and location as input for the MODTRAN radiative transfer code and a suite of integrative algorithm to infer the up-welling, down-welling radiances and site-specific transmission. Land surface emissivity values are to acquire by virtue of the NDVI threshold method (Sobrino *et al.* 2004). The data used in the research were from the Thematic Mapper (TM) sensor on board Landsat 5 during the period of February 3, 2000 to December 31, 2010. TM data have six spectral bands with different spatial resolution, i.e., 30-m resolution for bands 1-5 and 7, and 120-m resolution for band 6 (TIR band). The level L1T product was downloaded from the Landsat archive at the USGS Earth Resources Observation and Science Center website. Only clear-sky images for the study area are chose for further analysis. The acquired images from path 41, row 36 and path 41, row 37 were first mosaicked and then subset to the study area. Eventually, a total of 82 scenes available from the Landsat archive were utilized for the analysis. The mean acquisition time was 18:13 PM UTC (10:13 AM local time) with the standard deviation of 6 min, indicating the images were recorded at the time of temperature rapid increase. The monthly distribution of image scenes is illustrated in Fig. 3-2.

These scenes were also grouped by season: winter (December- February: 15 scenes), spring (March-May: 22), summer (June-August: 25), and autumn (September-November: 15). The original images were first cropped into the study area and projected to UTM coordinate system (UTM, Zone N 11) before subsequent processing.

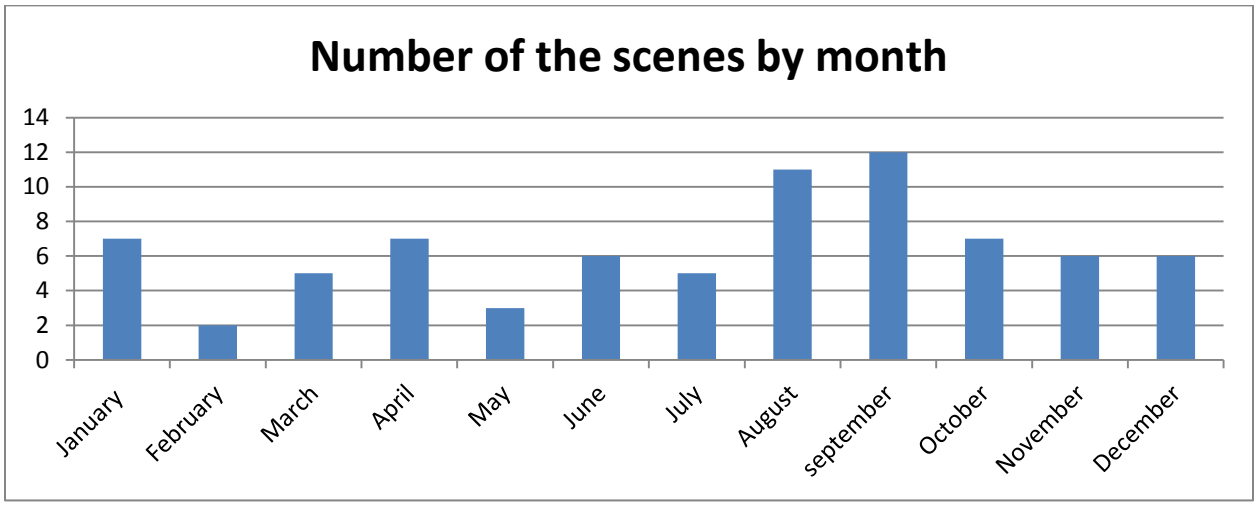

Figure 3- 2 The number of the image scene collected grouped by month

Another data source used for the research to test the efficiency of the proposed decomposition method comes from the data simulation. The simulation strategy introduces changes in seasonal and trend components with different levels of noise. Simulated LSTs will be generated by summing individually simulated seasonal, trend, and noise components. The seasonal component is produced by a sinusoidal model with changes in amplitude and angular frequency. The stochastic item is created by using a random number generator that follows a normal distribution N ($\mu=0$, $\delta=x$). Finally, different percent (up to 50%) of the simulated LST time series data points will be removed to keep the consistence with the real observations.

CHAPTER 4

METHODOLOGY

Urbanization related activities inevitably alter the natural environment, resulting in corresponding changes in climate variables, including LSTs. Consequently, it is expected that

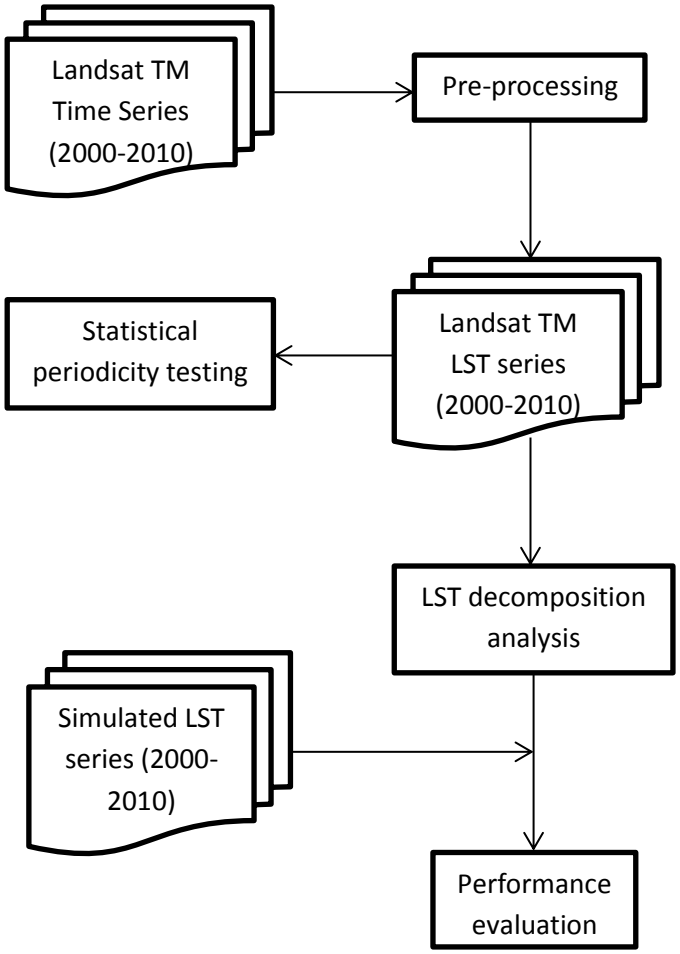

Figure 4- 1 Specific procedures for proposed study.

urbanization process, to some degree, wreaks havoc on the landscape thermal patterns. Furthermore, at the global scale, it is obvious that global warming is happening although the specific warming trend is still uncertain and obscured. Then it is evident that there is an increasingly rapid growth for urbanization and the rapid development has been accused of accounting for local, regional and even global climate change. Therefore, it is of important necessity to conduct the statistical hypothesis testing for LST periodicity and to decompose long-term LST observations. The flowchart in Fig. 4-1 shows the specific procedures for this proposed study. First, acquired TM time series data are subject to the pre-processing, including subset, atmospheric calibration, and computation of LSTs. Then the derived LST time series will be analyzed by using the Lomb-Scargle periodogram technique and by using the proposed decomposition method. The performance of the new decomposition method is evaluated by virtue of simulated LST observations. Section 4.1 and section 4.2 will present the statistical hypothesis testing technique and the decomposition method, respectively.

4.1 Statistical hypothesis testing for periodicity using Lomb–Scargle periodogram

Although visually rhythmic patterns within LST variations have been known for over decadal years, yet there still lacks detailed statistical analysis and evidence for confirmation. This situation is further acerbated by the unevenly distributed time series data, positing a challenge to search for the periodicity. In this research, we propose to use the Lomb–Scargle periodogram for the statistical hypothesis testing and for searching for possible periodic components. For a LST value at a pixel observed at time t_i, we denote that the time series by $Y(t_i)$ for $i = 1, 2, 3, \ldots N$. To model $Y(t_i)$ for periodicity, we have

$$Y(t_i) = S(t_i) + \varepsilon(t_i) \dots\dots\dots\dots\dots\dots\dots (2)$$

Where $S(t_i)$ is a periodic function with a positive period T such that $S(t_i) = S(t_i + T)$ for all t_i; and $\varepsilon(t_i)$ is assumed as a sequence of norm random errors with mean 0 and homogeneous variance (Scargle 1982). Unlike the Fourier Transform, in which the Fourier frequencies are used, it is assumed that there are M test frequencies $f_1, f_2, \dots, f_M$ and their corresponding angular frequencies are $\omega = 2\pi f_j$, for $j = 1, 2, \dots, M$. The Lomb-Scargle periodogram is defined by Press &Rybicki (1989) as equation (3).

$$P(\omega_j) = \frac{1}{2\sigma^2}\left\{\frac{\left(\sum_{i=1}^{N}[y(t_i) - \bar{y}]\cos[\omega_j(t_i - \tau)]\right)^2}{\sum_{i=1}^{N} cos^2[\omega_j(t_i - \tau)]} + \frac{\left(\sum_{i=1}^{N}[y(t_i) - \bar{y}]\sin[\omega_j(t_i - \tau)]\right)^2}{\sum_{i=1}^{N} sin^2[\omega_j(t_i - \tau)]}\right\} \dots (3)$$

With τ defined by

$$\tan(2\omega_j\tau) = \frac{\sum_{i=1}^{N}\sin(2\omega_j t_i)}{\sum_{i=1}^{N}\cos(2\omega_j t_i)}$$

And

$$\bar{y} = \frac{1}{N}\sum_{i=1}^{N} y(t_i)$$

$$\delta = \frac{1}{N-1}\sum_{i=1}^{N}[y(t_i) - \bar{y}]$$

The null distribution of the Lomb-Scargle periodogram $Z_j = P(\omega_j)$ at a given frequency ω_j is exponentially distributed (Scargle 1982), i.e., the cumulative distribution function is

$$F(z) = P(Z_i < z) = 1 - e^{-z} \dots\dots\dots (4)$$

For the present study, the null hypothesis is LST time series is non-periodic versus the alternative one that it is periodic. Thus, the observed statistical significance level, the p-value, of testing the

null hypothesis that such a peak in Lomb-Scargle periodogram is due to chance is calculated by equation (5) suppose there are M independent frequencies.

$$\Pr = p - value = 1 - (1 - e^{-z})^{M} \ldots\ldots\ldots (5)$$

With the above steps, it is possible to identify periodic patterns claimed to show statistically significant level for a given false discovery rate (FDR) *q*.

4.2 LST decomposition

The decomposition of LST time series allows a closer examination of thermal dynamics caused by human disturbances. A breakdown scheme proposed here is to disassemble observed records into a seasonal, a trend, and a remainder component, respectively. The procedure to estimate each component is described as below for irregularly spaced time series data.

Consider a time series *Y* in the form described by equation (6). M represents the deterministic trend and *R* is a stationary stochastic process with mean zero. To extract the trend, a local linear regression scheme based on the kernel smoothing (i.e., a weighting function) is adopted given the boundary data effect (Hastie *et al.* 2001). For a consistent time series, this local kernel regression is adequate in isolating the trend change; however, an irregularly spaced time series requires additional efforts to consider the impacts of different observations intervals on trend extraction. Here a further weighting function is proposed for optimization showed in equation (7).

$$Y(t_i) = M(t_i) + R(t_i) \dots\dots\dots (6)$$

$$\omega(t_i) = \frac{1}{2d}\begin{cases} t_{i+1} - t_i, if\ 1 < i < N \\ t_2 - t_1, if\ i = 1 \\ t_N - t_{N-1}, if\ i = N \end{cases} \dots\dots\dots\dots (7)$$

With *d* the normal observation interval (for Landsat time series, *d* is 16), and *N* is the number of the observations. The weighting function is inversely related to observation density.

The seasonal estimation is based on the study by Eckner (2012) using the averaging of subintervals method. Suppose a time series in the form described by equation (8).

$$Y(t_i) = S(t_i) + R(t_i) \dots\dots\dots (8)$$

$S(t_i)$ represents the seasonal component with period *l* present in the time series *Y*. Then the seasonal item is extracted via equation (9).

$$S = avg[Y(r): r \in (\min(t_i), \max(t_i)), \varphi(r) = t] \dots\dots\dots (9)$$

Where φ denotes the function that maps a time point to its relative position within the period for $0 \leq t \leq l$. It is usually necessary to drop a sampled value $Y(r)$ from the calculation of the average if the associated time point *r* is not close to any observation time of *Y*. Otherwise, linear interpolation would "trim down the valleys and fill in the troughs" of seasonal fluctuations (Eckner 2012).

For the present research, we propose to decompose the LST time series into seasonal, trend, and remnant components specified by equation (10) for multi-timescale analysis. An iterative scheme should be developed for jointly isolating each component. Detailed procedures include: 1) initializing the *S* item with 0; 2) estimating the trend of *Y-S* using the local linear regression above; 3) estimating the seasonality of *Y-M* using the averaging of subintervals method; 4) repeating the step 2) and 3) until no changes in the *S* and *M*, i.e., a convergence is reached.

$$Y(t_i) = S(t_i) + M(t_i) + R(t_i) \dots\dots\dots (10)$$

Then the proposed decomposition method is applied to both the simulated LST time series and real observed Landsat satellite images for further quantitative analysis.

CHAPTER 5

RESULTS ANALYSIS

5.1 Rhythmic patterns analysis

The application of the Lomb–Scargle periodogram to the time series LST images produced estimates of power density, periodic frequency, and the corresponding statistical significance level for individual pixels. The power density is defined in equation (3), which makes the periodogram analysis invariant to the shift of the origin time and equivalent to the least square fitting process (Hornes & Baliunas 1986). To illustrate the usefulness of the three parameters in analyzing the periodic patterns of LST time series, a urban pixel with UTM coordinate (3865953.603, 3751873.495, unit in meters) was selected and the corresponding LST values and periodogram results were shown in Figure 5-1.

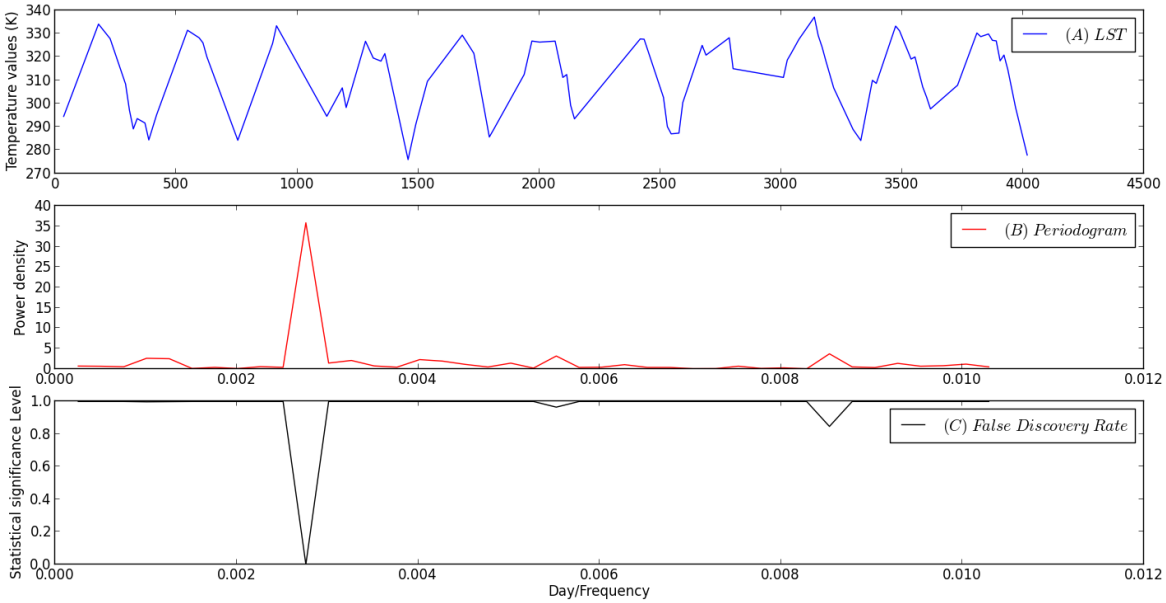

Figure 5- 1 The LST observations (A) and the corresponding Periodogram results including the power density (B) and the False Discovery Rate (C).

Panel (A) displayed the LST variations between 2000 and 2010. Since the defined power density was invariant to the origin of the time, the first day of 2000 was considered as day 1, from which the day numbers for different images were calculated. Based on the fact that the Landsat revisit time is 16-day, the maximum frequency for the periodogram analysis was set up to 0.03125 (1/32), the sampling Nyquist frequency to reduce confusion. However, for the present study, this option seemed to be not necessary since the derived periodogram results only provided frequency up to around 0.011. This was due to the inherent capability of Lomb-Scargle technique to determine the frequency range under the limit of the maximum frequency. In the Panel (B), obviously, there are several local peaks occurring at frequency 0.00275 (period 362), 0.00552 (period 181), and 0.00853 (period 117). These three peaks were meaningful because these three periodic times were essentially consistent with annual (1/365), semi-annual (2/365), and seasonal-like LST dynamics (3/365). Another reason for the interests in the three periodic times was that the Panel (C) provided the matching downward peaks for the statistical

significance values although the last two periodic times should be rejected at a given significance level either of 0.05 or 0.01. Nevertheless, since the Lomb-Scargle is a statistical hypothesis testing technique, the rejection did not mean that there were not semi-annual and seasonal-like variations within the time series LSTs. In contrast, the derived results merely showed that LST observations did not provide strong evidence for determining the semi-annual and seasonal-like variations. It could be concluded that the obtained 82 time series were not adequate in studying semi-annual and seasonal-like variations. The results from the application of the Lomb-Scargle analysis to all pixels of the study area suggested the same conclusion that the 82 LST images could be used for isolating the annual variations at the significance level of 0.01 with a period time of 362.18 days and that there was no strong evidence to demonstrate the semi-annual and seasonal-like dynamics.

Compared to the study conducted by Weng & Fu (2014), the difference was that the assumed annual temperature cycle was 365 days rather than the identified 362.18 days in the present research. To determine whether the difference was caused by data missing or was limited by the Landsat revisit intervals, the simulated annual LST time series variations with the periodic time of 365 days were employed. Without clouds or poor atmospheric conditions, the used time series data would have roughly 250 images scenes over decadal years. Therefore, the Lomb-Scargle analysis utilized the simulated 250 LST time series with interval of 16-day to illustrate the tolerance of the technique to the data missing. The amplitude for the annual dynamics and the mean annual surface temperature were set at 15 K and 295 K, respectively. Table 5-1 showed the tolerance of the Lomb-Scargle technique to data missing, ranging from 20 to 190. The number of images less than 60 is not considered since the identified periodic time decrease greatly after that. Overall, the detection capability of the periodogram technique decreased with the increased

number of missing data observations as evident in the table results of the *Periodic time*. The exception occurred to the number of 70 or 60 images, which was probably due to the robustness of the Lomb-Scargle analysis, which preserves the periodic identification ability even with a small number of temperature observations. Therefore, the difference of the annual temperature periodic time between the study of Weng & Fu (2014) and the present research was attributed to the data missing caused by clouds contamination and/or poor atmospheric conditions.

Table 5- 1 The tolerance of the Lomb-Scargle technique to data missing

Image Number	250	230	210	190	170	150
Periodic time	365.0	364.8	364.5	364.1	363.7	363.1
Image Number	130	110	90	80	70	60
Periodic time	362.5	361.59	360.8	360.2	360.6	360.9

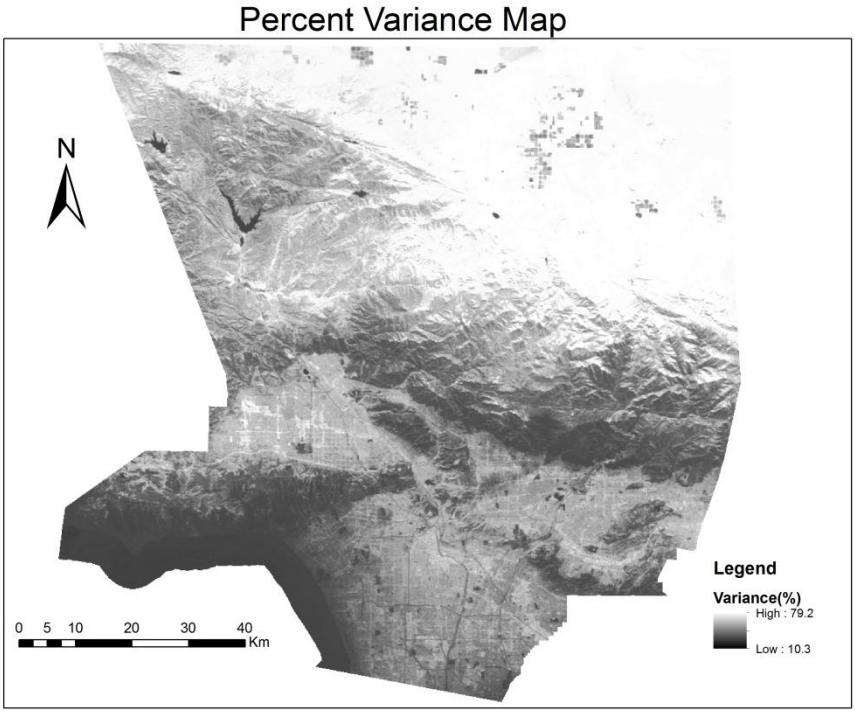

Figure 5- 2 The percent variance map explained by the identified annual temperature cycle over 2000-2010

Figure 5-2 revealed the percent variance map by which the identified periodic patterns would explain for the decadal years LST dynamics. To facilitate the variance computation, the

sinusoidal function was assumed and employed. The resultant variance image of figure 5-2 was multiplied by 100 to display the percent variance. Overall, it was evident that there was an increase trend for the percent variance as the latitude increased. However, the study area is not big enough to accommodate too many changes of ocean climatic effects. Thus, the observed variance patterns could be attributed to the geographic location of the study area, i.e., the land cover and land use composition. In addition, a low percent variance could be observed in vegetated areas, suggesting the impact of vegetation on surface temperature fluctuations. From the perspective of surface energy balance, the vegetation acted on LST mainly through latent fluxes, and this process generated extra complexity for temperature variations that may not be identified as the periodic pattern from the remote sensing perspective. In the urban areas, mainly the southern part of the study area, the percent variance was also relatively low with the mean value of the percent variance of 25.3. Although the low value could be explained by the effects of the sea breeze, it was reasonable to assume that the urbanization may have produced its own temperature pattern compared to other land covers, thus lowering the variance explained by the isolated rhythmic pattern. As such, urbanization could be regarded as to weaken the annual temperature dynamics by producing urbanization associated LST variations. High percent variance mainly occurred in the northern and northeastern part of the study area, from which the Mojave Desert / barren land stretched westward. This phenomenon revealed that surface compositions could impact the temperature patterns and the corresponding acting force magnified with the increased complexity of surface fabrics given the comparisons of materials between urban and barren land regions. The inland water region displayed a low percent variance due to the high thermal capacity of water to resist temperature changes and/or energy exchange between water and the surrounding land cover and or atmosphere, thus creating non-annual

temperature distributions and reducing the percent variance. Therefore, it could be concluded that the variance explained by the identified periodic pattern in the study area was subject to surface compositions. More importantly, urbanization generated additional LST variations, thus weakening the annual surface temperature dynamics evident by the low value of the percent variance explained by the annual temperature dynamics.

5.2 Decomposition analysis

5.2.1 Test of the decomposition technique by simulated LST data

Since there was not any field observed data available, the validation of the decomposition technique was implemented by using simulated LST consisting of seasonality, trend, and noise components. The specific parameters for the three components were listed in table 5-2. Figure 5-3 showed the results derived from the application of the iterative decomposition technique to the simulated LST. Only results for amplitude of 15 K and trend of 0.1 K per year were summarized in the figure since similar results were obtained for other amplitude and trend values. The seasonality estimation errors were also not showed in the figure since the estimated seasonality error was always below 0.1 by using the different noise level and different preserved point number of points. Therefore, the seasonality component estimation was not subject to the noise level and the number of points used in decomposition process. As illustrated from figure 5-3, the estimation of trend component was influenced by the noise level and the corresponding errors in trend component increased as the noise level expanded. The preserved number of points also impacted the performance of the decomposition technique. This was reasonable since the missing of data points could obscure the temperature dynamics thus magnifying the absolute errors. Finally, the estimation of the seasonal component did not affect the derivation of trend

variations. Figure 5-3 also showed that the impact of the combination of the preserved number of points and the noise level on the absolute difference was up to 0.06 K, 60% percentage of the simulated trend per year. Overall, figure 5-3 illustrated that the absolute difference increased slowly as the noise level and the missing of data points increased.

Table 5- 2 Parameter values for simulating LST time series

Parameters	Values
Seasonality (Amplitude)	15, 20
Trend (change/per year)	0, 0.1, 0.2
Noise (variance δ^2)	1, 2, 3, 4, 5
Preserved point number*	150, 130, 110, 90, 70

* Initially the simulated LST time series have 250 observations.

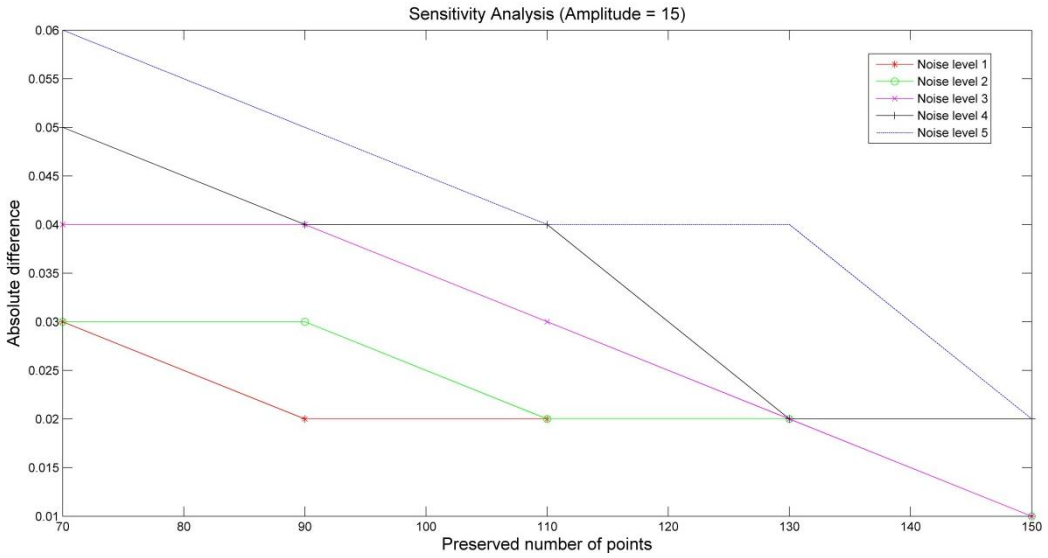

Figure 5- 3 The sensitivity analysis of the decomposition technique by using simulated LSTs (Amplitude = 15, Trend = 0.1/per year). The preserved number of points represented the number of points used in the decomposition process. The absolute error was used to measure the errors in estimated trend component compared to the simulated trend.

5.2.2 Application of the decomposition technique to remote sensing data

Since the iterative algorithm requires a long computation time for each pixel, it should be better for the comparison analysis between urban and non-urban regions by creating mean/median composite. Moreover, the composite data could also further eliminate/remove some of the noised pixels produced in the LST computation. In this study, the NLCD 2006 was employed and the median composite LSTs were created for each land cover. Figure 5-4 provided the decomposition results derived from the application of the decomposition technique to remote sensing data for each land cover. In terms of seasonality component, it should be explained in the way in which the temperature increased by a number based on the corresponding trend component.

The amplitudes of the seasonality for individual land covers were successfully retrieved, i.e., 3.0 K (water), 18.8 K(developed), 22.7 K(barren), 16.4 K(forest), 17.8 K(shrubland), 21.5 K(herbaceous), 20.7 K(planted/cultivated), and 15.4 K (wetlands). These results are comparable to the study of Weng & Fu (2014). As in the sensitivity test, the seasonality component could be estimated robustly. Overall, the estimated seasonality amplitude corresponded well to each land cover. Therefore, for a simplified analysis of annual temperature dynamics, a sinusoidal model was adequate.

The trend component could be considered as the inter-annual change or the temperature variations (increase or decrease) over decadal years. Land covers of developed, barren, forest, shrubland, and wetlands displayed an increase pattern with temperature increases of 1.2 K, 0.5 K,

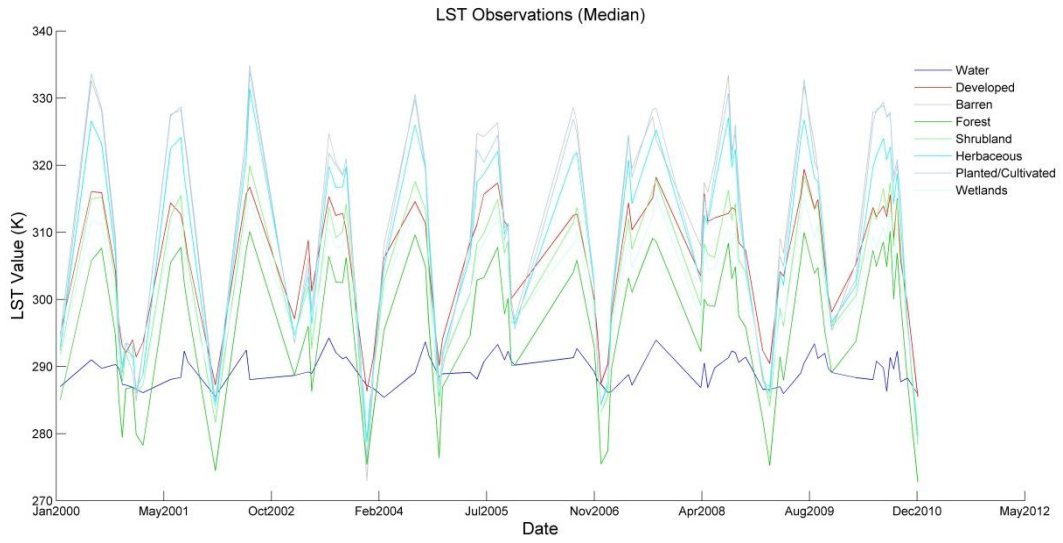
LST Observations (Median)
LST Value (K)
Date
Water
Developed
Barren
Forest
Shrubland
Herbaceous
Planted/Cultivated
Wetlands
340
330
320
310
300
290
280
270
Jan2000
May2001
Oct2002
Feb2004
Jul2005
Nov2006
Apr2008
Aug2009
Dec2010
May2012

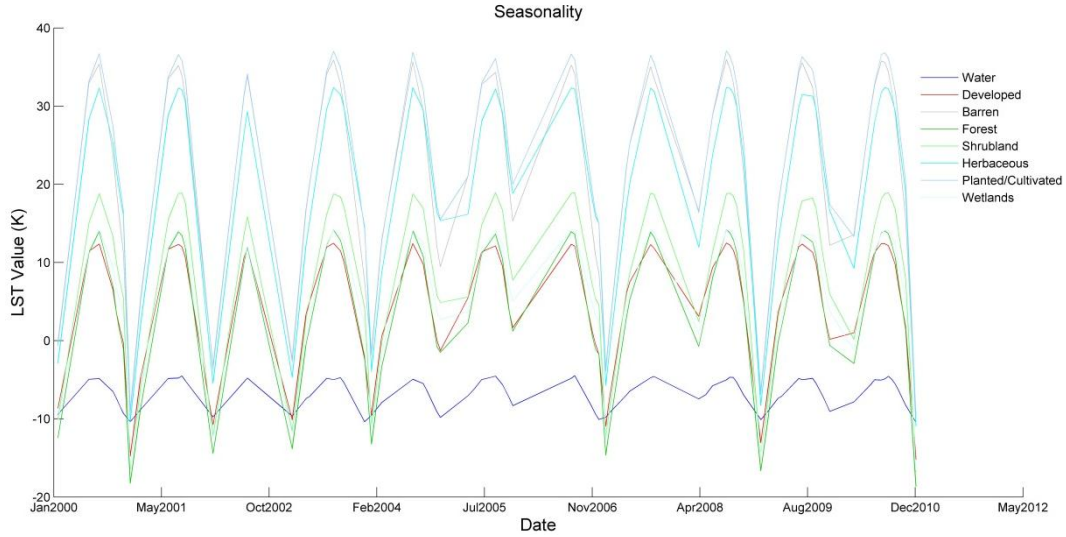
Seasonality
LST Value (K)
Date
Water
Developed
Barren
Forest
Shrubland
Herbaceous
Planted/Cultivated
Wetlands
40
30
20
10
0
-10
-20
Jan2000
May2001
Oct2002
Feb2004
Jul2005
Nov2006
Apr2008
Aug2009
Dec2010
May2012

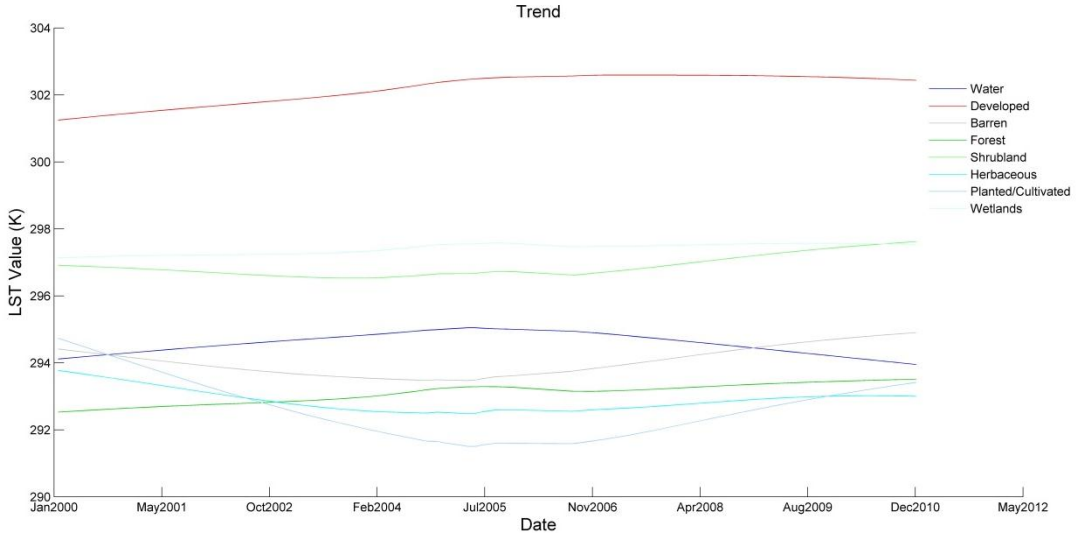
Trend
LST Value (K)
Date
Water
Developed
Barren
Forest
Shrubland
Herbaceous
Planted/Cultivated
Wetlands
304
302
300
298
296
294
292
290
Jan2000
May2001
Oct2002
Feb2004
Jul2005
Nov2006
Apr2008
Aug2009
Dec2010
May2012

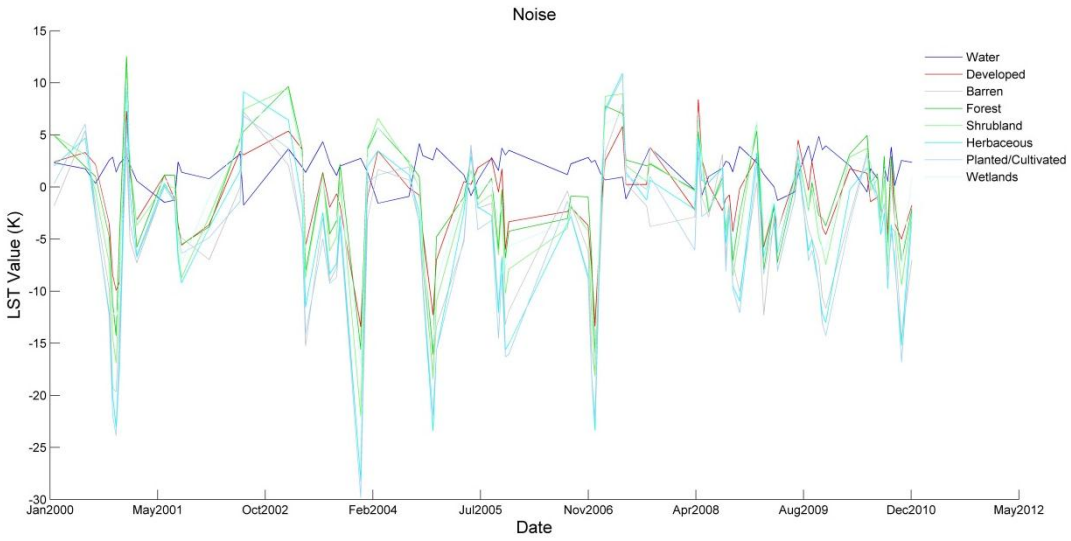

Figure 5- 4 Application of the decomposition technique to individual land covers including water, developed, barren, forest, shrubland, herbaceous, planted/cultivated, and wetlands. In each panel, the figure showed the original median LST observations, decomposed seasonality, trend, and noise components.

1.0 K, 0.7 K, 0.4 K respectively over decadal years (temperature in 2010-temperature in 2000). In contrast, the remaining land covers, including water, herbaceous, and planted, showed a temperature decrease trend -0.2 K, -0.8 K, and -1.3 K, respectively. The existence of positive and negative trend change values may suggest different variation patterns for different land covers and could possibly attribute to the fact that only 10 years' remote sensing data was used for analysis which may partly obscure the trend change. However, even with the land covers showing a temperature decrease from 2000 to 2010, it could be observed from the trend component that there was an increase in LST. It seemed that year 2004-2005 was a time period in which the trend began to increase or decrease, suggesting either some climatic events in the period or the inter-annual change may also showed a periodic pattern, not captured by the annual temperature dynamics, or merely a non-periodic pattern. Therefore, for the ease of the trend

comparisons between urban and non-urban regions, only land covers showing a consistent increase change were selected and eventually the land covers of developed and forest and wetlands were used for the comparisons. In these three land covers, the developed regions revealed the highest trend change over the ten years, and showed a range of 0.2 K to 0.8 K difference compared to the other two land covers, suggesting that the urbanization associated land covers may further create a trend change rather than the already known climate change. Furthermore, it should be noted that the reason for not using other land covers as comparison basis was because they did not uncover a consistent trend change and should be explored in a much longer period to check if the inter-annual change showed a periodic or non-periodic pattern. Thus the temperature increase or decrease change could be confirmed and could be used for the comparison of urban and non-urban regions to show the possible trend variations caused by urbanization. In the present study, it was concluded that the urbanization associated land cover created a trend change pattern ranging from 0.2 K to 0.8 K. The noise component should be regarded as the weather impacts on temperature changes. Further analysis suggested that the noise component resolved around the zero line, indicating that the extracted seasonality and trend components could well represent the temperature dynamics. As such, the noise component could also be assumed as a way to measure the efficiency and robustness of the decomposition technique, especially when the validation data was missing.

CHAPTER 6

DICUSSIONS & FUTURE WORK

The major contribution of the thesis research is to provide the statistical evidence of the existence of the rhythmic patterns and the decomposition technique for the obtained evenly distributed time series data. The main characteristics of the Lomb-Scargle periodogram and the proposed decomposition technique are both revealed by using simulated LST data consisting of either the seasonality or the combination of the seasonality, trend, and noise components. The lomb-Scargle periodogram is a statistical hypothesis technique with the assumption that the null distribution of each frequency is exponentially distributed and its corresponding application is only subject to the extent to which the time series data is unevenly distributed. Previous studies in Bechtel (2012) and Weng & Fu (2014) showed that the annual temperature cycle (ATC) was adequate in studying urban thermal patterns; however, statistical evidence was lacking to explain why such an ATC exists.

The decomposition technique is developed mainly for analyzing to what degree the urbanization impacts the surface thermal properties. Simulation of LST time series data illustrated that the proposed technique was influenced by the noise level and the preserved number of point of the observations. Nonetheless, the derivation of LST from NASA Correction Parameter Calculator (Barsi et al. 2005) reported an error of ± 1K, which at most results in,

according to the sensitivity analysis of the decomposition technique, 30% biases in estimating the trend component when the time series data is seriously unevenly distributed (only 70 points). The biases can be further attenuated in this study since it focused on the comparisons between urban and other land cover regions. The most important contribution of this iterative technique is its ability to break down the time series data into seasonality (annual change) and trend (intra-annual change) components, facilitating the study of the impacts of urbanization. Considerations for further research can be fallen into several aspects:

1) The proposed Lomb-Scargle technique can be used for studying the periodic patterns involved in other biophysical parameters, such as NDVI and LAI, and even data from MODIS time series. The critical point is that the periodogram analysis cannot only detect annual change, but also shows potential to isolate the periodic patterns at intra-annual (less than a year) and inter-annual (more than a year) temporal scales depending on the availability of the data. Despite the robustness of the technique, it is still necessary to obtain as much time series data as possible to reduce the possible calculation biases. If some of the biophysical parameters only show different periodic patterns, they could be reconstructed from the remote sensing observations at even finer scales, such as from 16 days (Landsat revisit frequency) to a daily basis. The application of the proposed method would be very useful especially for some areas experiencing severe clouds days.

2) Further application of the decomposition technique should work with an even longer period of time series LSTs to confirm the LST changes attributed to urbanization other than the changes caused by the already known global climate change. Up until now, it is still uncertain about whether urbanization results in regional and/or global climate change. However, the thesis research does show a higher trend component in urban regions compared to the regions (forest

and wetlands) showing consistent increase trend variations. The remaining land covers does not show a consistent increase or decrease patterns, probably suggesting either a periodic pattern at an intra-annual scale or a non-periodic pattern showing some climate events that needs to be further considered and explored. Therefore, the alternative can be to employ the Landsat TIR data obtained since 1982 for the decomposition analysis. Currently, the only problem is the lack of standardized LST product from the Landsat archive despite the availability of other Landsat products, such as surface reflectance climate data record (CDR) and surface derived indices. The way to compute LSTs using the NASA Correction Parameter Calculator can only be applied to the Landsat data after 2000 (Barsi et al. 2005) due to the lack of atmospheric profiles. The promising aspect is that such a LST product is in progress (Schott *et al*. 2012) and thus the decomposition technique is expected to further confirm the climate change attributed to urbanization with the upcoming Landsat LST product. In addition, the iterative decomposition technique assumes that the seasonality component should be time constant and there is no intra-annual change for the seasonality component. Such an assumption can be held over a decadal year since only ten years data does not allow the discrimination of the change of seasonality. However, if more than one decadal years LST data is utilized, it will become obvious that the seasonality component is time-varying. The noteworthy point is that the proposed decomposition technique has the capacity to absorb a time varying seasonality component as long as the locally weighted scatterplot smoothing (LOWESS) scheme is employed in the seasonality estimation described in equation (9).

3) The proposed decomposition technique illustrates potentials in the continuous change detection and classification of land covers (Zhu & Woodcock, 2014). In the study of Zhu & Woodcock (2014), they utilized a parametric model comprising seasonality, trend, and break

components to estimate reflectance and brightness temperature for the detection of land cover change. Then the land cover classification is realized through the Random Forest Classification with inputs from the coefficients of the time series model. The same scheme can also be employed by using the proposed decomposition technique. Therefore, the operation can be performed on a pixel basis rather than using the median composite present in this thesis research. As to the difference between the proposed decomposition technique and the parametric model used in Zhu & Woodcock (2014), further comparisons will be done in terms of land cover change detection.

Despite the mentioned promising aspects, further considerations should be directed to the possible biased introduced from the factors of elevation and inherent thermal anisotropy characteristics. The elevation influence was evident since apparently the percent variance map of figure 5-2 showed the hilly shade effects. Given that the LST is an anisotropy parameter, the combined effect of the elevation and thermal anisotropy on the multi-timescale analysis may be more complicated. Furthermore, the thesis research aimed at analyzing dynamics of the unevenly distributed LST time series data and at how the remotely sensed data could help illustrate the impact of the urbanization on surface thermal properties. Therefore, the results need to be further confirmed by investigating the linkages between the urban developments and the surface thermal properties. Future directions can be placed on correlating the urban morphology and compositions with the time series data to illustrate the interactive aspects between urbanization and surface thermal properties. Hopefully, the causes and consequences of the surface thermal property changes can be revealed and effective measures can be taken for future environmental sustainability.

CHAPTER 7

CONCLUSIONS

The thesis research aims at analyzing the impacts of urbanization on the surface thermal properties, i.e., the LST dynamics over decadal years by using Landsat TM LST data. To our knowledge, the existence of the periodic pattern in the LST dynamics is first confirmed in the presented study from a statistical perspective although previous studies illustrated the suitability of an ATC model to characterize thermal patterns. By using simulated LST data consisting of only the seasonality component, the robustness of the Lomb-Scargle periodogram technique is illustrated and the corresponding application is influenced by the preserved number used in the computation. The error for the frequency estimation of the rhythmic patterns can be up to 5 days following the decrease of available time series data. The analysis of variance explained by the assumed annual temperature cycle showed a percent mean variance value of 25.3 in urban regions, a relatively low value compared to other natural land covers, suggesting a weakened annual temperature cycle caused by the urbanization as expected from the hypothesis.

The iterative decomposition technique consisting of seasonality, trend, and noise components provides a specific way to measure the influence of urbanization in the LST variations. The sensitivity analysis of the decomposition technique suggests the robustness of the break-down scheme and indicates that the estimation of seasonality is not influenced by the preserved number of points and noise level whereas the trend estimation can be affected by both

factors and the total combined error can be up to 0.06 K per year for trend component estimation. Further comparison analysis of the trend component among different land covers, i.e., urban and non-urban regions, indicated that urbanization would cause climate change circa 0.2-0.8 K. Future work will be directed to the further confirmation of the urbanization related climate change by utilizing several decades' LST data from all the available Landsat TIR data.

References

Anderson, M. C., Allen, R. G., Morse, A. & Kustas, W. P. (2012). "Use of Landsat thermal imagery in monitoring evapotranspiration and managing water resources." *Remote Sensing of Environment* 122: 50-65.

Anderson, M. C., Kustas, W. P., Norman, J. M., Hain, C. R., Mecikalski, J. R., Schultz, L., Gonzalez-Dugo, M. P., Cammalleri, C., d'Urso, G., Pimstein, A. & Gao, F. (2011). "Mapping daily evapotranspiration at field to continental scales using geostationary and polar orbiting satellite imagery." *Hydrology and Earth System Sciences* 15(1): 223-239.

Barsi, J. A., Schott, J. R., Palluconi, F. D. & Hook, S. J. (2005). "Validation of a web-based atmospheric correction tool for single thermal band instruments." Proc. SPIE 5882, Earth Observing Systems X, 58820E (September 07, 2005); doi:10.1117/12.619990.

Bechtel, B. (2012). "Robustness of Annual Cycle Parameters to Characterize the Urban Thermal Landscapes." *Geoscience and Remote Sensing Letters, IEEE* 9(5): 876-880.

Becker, F., Li, Z. & Mather, P. (1992). "Temperature-independent thermal infrared spectral indices and land surface temperature determined from space." *TERRA-1: understanding the terrestrial environment: the role of earth observations from space.*: 185-201.

Berk, A., Bernstein, L. S. & Robertson, D. C. (1987). MODTRAN: A moderate resolution model for LOWTRAN, DTIC Document.

Buyantuyev, A. & Wu, J. G. (2010). "Urban heat islands and landscape heterogeneity: linking spatiotemporal variations in surface temperatures to land-cover and socioeconomic patterns." *Landscape Ecology* 25(1): 17-33.

Chen, J., Jonsson, P., Tamura, M., Gu, Z. H., Matsushita, B. & Eklundh, L. (2004). "A simple method for reconstructing a high-quality NDVI time-series data set based on the Savitzky-Golay filter." *Remote Sensing of Environment* 91(3-4): 332-344.

Chen, X. L., Zhao, H. M., Li, P. X. & Yin, Z. Y. (2006). "Remote sensing image-based analysis of the relationship between urban heat island and land use/cover changes." *Remote Sensing of Environment* 104(2): 133-146.

Dash, P., Gottsche, F. M., Olesen, F. S. & Fischer, H. (2005). "Separating surface emissivity and temperature using two-channel spectral indices and emissivity composites and comparison with a vegetation fraction method." *Remote Sensing of Environment* 96(1): 1-17.

Deng, C. B. & Wu, C. S. (2013). "Examining the impacts of urban biophysical compositions on surface urban heat island: A spectral unmixing and thermal mixing approach." *Remote Sensing of Environment* 131: 262-274.

Dominguez, A., Kleissl, J., Luvall, J. C. & Rickman, D. L. (2011). "High-resolution urban thermal sharpener (HUTS)." *Remote Sensing of Environment* 115(7): 1772-1780.

Dousset, B. & Gourmelon, F. (2003). "Satellite multi-sensor data analysis of urban surface temperatures and landcover." *ISPRS Journal of Photogrammetry and Remote Sensing* 58(1-2): 43-54.

Dozier, J. (1981). "A method for satellite identification of surface temperature fields of subpixel resolution." *Remote Sensing of Environment* 11: 221-229.

Eckner, A. (2012). " A Note on Trend and Seasonality Estimation for Unevenly-Spaced Time Series." http://www.eckner.com/papers/trend_and_seasonality.pdf.

Friedl, M. A. (2002). "Forward and inverse modeling of land surface energy balance using surface temperature measurements." *Remote Sensing of Environment* 79(2-3): 344-354.

Gao, F., Kustas, W. & Anderson, M. (2012). "A Data Mining Approach for Sharpening Thermal Satellite Imagery over Land." *Remote Sensing* 4(11): 3287-3319.

Gillespie, A., Rokugawa, S., Matsunaga, T., Cothern, J. S., Hook, S. & Kahle, A. B. (1998). "A temperature and emissivity separation algorithm for Advanced Spaceborne Thermal Emission and Reflection Radiometer (ASTER) images." *IEEE Transactions on Geoscience and Remote Sensing* 36(4): 1113-1126.

Gillespie, A. R. (1986). Lithologic mapping of silicate rocks using TIMS. The TIMS Data User's Workshop p 29-44(SEE N 87-17111 09-43).

Gillespie, A. R. (1992). "Spectral Mixture Analysis of Multispectral Thermal Infrared Images." *Remote Sensing of Environment* 42(2): 137-145.

Gottsche, F. M. & Olesen, F. S. (2001). "Modelling of diurnal cycles of brightness temperature extracted from METEOSAT data." *Remote Sensing of Environment* 76(3): 337-348.

Grimm, N. B., Faeth, S. H., Golubiewski, N. E., Redman, C. L., Wu, J. G., Bai, X. M. & Briggs, J. M. (2008). "Global change and the ecology of cities." *Science* 319(5864): 756-760.

Harlan, S. L., Brazel, A. J., Prashad, L., Stefanov, W. L. & Larsen, L. (2006). "Neighborhood microclimates and vulnerability to heat stress." *Social Science & Medicine* 63(11): 2847-2863.

Hastie, T. J., Tibshirani, R. J. & Friedman, J. J. H. (2001). The Elements of Statistical Learning: Data Mining, Inference, and Prediction, Springer-Verlag.

Hornes, J. H., Baliunas, S. L. (1986). " A prescription for period analysis of unevenly sampled time series." *Astrophysical Journal, Part 1* 302: 757-763.

Imhoff, M. L., Zhang, P., Wolfe, R. E. & Bounoua, L. (2010). "Remote sensing of the urban heat island effect across biomes in the continental USA." *Remote Sensing of Environment* 114(3): 504-513.

Inamdar, A. K. & French, A. (2009). "Disaggregation of GOES land surface temperatures using surface emissivity." *Geophysical Research Letters* 36(2).

Jeganathan, C., Hamm, N. A. S., Mukherjee, S., Atkinson, P. M., Raju, P. L. N. & Dadhwal, V. K. (2011). "Evaluating a thermal image sharpening model over a mixed agricultural landscape in India." *International Journal of Applied Earth Observation and Geoinformation* 13(2): 178-191.

Jimenez-Munoz, J. C. & Sobrino, J. A. (2003). "A generalized single-channel method for retrieving land surface temperature from remote sensing data." *Journal of Geophysical Research-Atmospheres* 108(D22), 4688, doi:10.1029/2003JD003480.

Ju, J. C. & Roy, D. P. (2008). "The availability of cloud-free Landsat ETM plus data over the conterminous United States and globally." *Remote Sensing of Environment* 112(3): 1196-1211.

Juarez, R. I. N. & Liu, W. T. (2001). "FFT analysis on NDVI annual cycle and climatic regionality in northeast Brazil." *International Journal of Climatology* 21(14): 1803-1820.

Keramitsoglou, I., Kiranoudis, C. T., Ceriola, G., Weng, Q. & Rajasekar, U. (2011). "Identification and analysis of urban surface temperature patterns in Greater Athens, Greece, using MODIS imagery." *Remote Sensing of Environment* 115(12): 3080-3090.

Kim, Y. H. & Baik, J. J. (2005). "Spatial and temporal structure of the urban heat island in Seoul." *Journal of Applied Meteorology* 44(5): 591-605.

Knapp, S., Kuhn, I., Stolle, J. & Klotz, S. (2010). "Changes in the functional composition of a Central European urban flora over three centuries." *Perspectives in Plant Ecology Evolution and Systematics* 12(3): 235-244.

Kustas, W. P., Norman, J. M., Anderson, M. C. & French, A. N. (2003). "Estimating subpixel surface temperatures and energy fluxes from the vegetation index-radiometric temperature relationship." *Remote Sensing of Environment* 85(4): 429-440.

Lafortezza, R., Carrus, G., Sanesi, G. & Davies, C. (2009). "Benefits and well-being perceived by people visiting green spaces in periods of heat stress." *Urban Forestry & Urban Greening* 8(2): 97-108.

Li, J. X., Song, C. H., Cao, L., Zhu, F. G., Meng, X. L. & Wu, J. G. (2011). "Impacts of landscape structure on surface urban heat islands: A case study of Shanghai, China." *Remote Sensing of Environment* 115(12): 3249-3263.

Liu, D. S. & Pu, R. L. (2008). "Downscaling thermal infrared radiance for subpixel land surface temperature retrieval." *Sensors* 8(4): 2695-2706.

Liu, H. & Weng, Q. (2012). "Enhancing temporal resolution of satellite imagery for public health studies: A case study of West Nile Virus outbreak in Los Angeles in 2007." *Remote Sensing of Environment* 117: 57-71.

Lu, D. S. & Weng, Q. (2004). "Spectral mixture analysis of the urban landscape in Indianapolis with landsat ETM plus imagery." *Photogrammetric Engineering and Remote Sensing* 70(9): 1053-1062.

Luck, M. & Wu, J. G. (2002). "A gradient analysis of urban landscape pattern: a case study from the Phoenix metropolitan region, Arizona, USA." *Landscape Ecology* 17(4): 327-339.

Martinez, B. & Gilabert, M. A. (2009). "Vegetation dynamics from NDVI time series analysis using the wavelet transform." *Remote Sensing of Environment* 113(9): 1823-1842.

McCloy, K. R. & Lucht, W. (2004). "Comparative evaluation of seasonal patterns in long time series of satellite image data and simulations of a global vegetation model." *IEEE Transactions on Geoscience and Remote Sensing* 42(1): 140-153.

Merlin, O., Duchemin, B., Hagolle, O., Jacob, F., Coudert, B., Chehbouni, G., Dedieu, G., Garatuza, J. & Kerr, Y. (2010). "Disaggregation of MODIS surface temperature over an agricultural area using a time series of Formosat-2 images." *Remote Sensing of Environment* 114(11): 2500-2512.

Oke, T. R. (1982). "The energetic basis of the urban heat island." *Quarterly Journal of the Royal Meteorological Society* 108(455): 1-24.

Oke, T. R., Zeuner, G. & Jauregui, E. (1992). "The Surface-Energy Balance in Mexico-City." *Atmospheric Environment Part B-Urban Atmosphere* 26(4): 433-444.

Ottle, C. & Stoll, M. (1993). "Effect of Atmospheric Absorption and Surface Emissivity on the Determination of Land-Surface Temperature from Infrared Satellite Data." *International Journal of Remote Sensing* 14(10): 2025-2037.

Paruelo, J. M. & Lauenroth, W. K. (1998). "Interannual variability of NDVI and its relationship to climate for North American shrublands and grasslands." *Journal of Biogeography* 25(4): 721-733.

Pettorelli, N., Vik, J. O., Mysterud, A., Gaillard, J. M., Tucker, C. J. & Stenseth, N. C. (2005). "Using the satellite-derived NDVI to assess ecological responses to environmental change." *Trends in Ecology & Evolution* 20(9): 503-510.

Prata, A. J. (1993). "Land-Surface Temperatures Derived from the Advanced Very High-Resolution Radiometer and the Along-Track Scanning Radiometer .1. Theory." *Journal of Geophysical Research-Atmospheres* 98(D9): 16689-16702.

Press, W. H. & Rybicki, G. B. (1989). "Fast algorithm for spectral analysis of unevenly sampled data." *The Astrophysical Journal* 338: 277-280.

Priestley, B. (1982). Spectral analysis and time series, Academic Press.

Qian, C., Fu, C. B. & Wu, Z. H. (2011). "Changes in the Amplitude of the Temperature Annual Cycle in China and Their Implication for Climate Change Research." *Journal of Climate* 24(20): 5292-5302.

Qin, Z., Karnieli, A. & Berliner, P. (2001). "A mono-window algorithm for retrieving land surface temperature from Landsat TM data and its application to the Israel-Egypt border region." *International Journal of Remote Sensing* 22(18): 3719-3746.

Rajasekar, U. & Weng, Q. H. (2009). "Urban heat island monitoring and analysis using a non-parametric model: A case study of Indianapolis." *ISPRS Journal of Photogrammetry and Remote Sensing* 64(1): 86-96.

Reisen, W., Lothrop, H., Chiles, R., Madon, M., Cossen, C., Woods, L., Husted, S., Kramer, V. & Edman, J. (2004). "West Nile virus in California." *Emerging Infectious Diseases* 10(8): 1369-1378.

Renzullo, L. J., Barrett, D. J., Marks, A. S., Hill, M. J., Guerschman, J. P., Mu, Q. Z. & Running, S. W. (2008). "Multi-sensor model-data fusion for estimation of hydrologic and energy flux parameters." *Remote Sensing of Environment* 112(4): 1306-1319.

Roerink, G. J., Menenti, M. & Verhoef, W. (2000). "Reconstructing cloudfree NDVI composites using Fourier analysis of time series." *International Journal of Remote Sensing* 21(9): 1911-1917.

Romero-Lankao, P., Qin, H. & Dickinson, K. (2012). "Urban vulnerability to temperature-related hazards: A meta-analysis and meta-knowledge approach." *Global Environmental Change-Human and Policy Dimensions* 22(3): 670-683.

Roth, M., Oke, T. R. & Emery, W. J. (1989). "Satellite-Derived Urban Heat Islands from 3 Coastal Cities and the Utilization of Such Data in Urban Climatology." *International Journal of Remote Sensing* 10(11): 1699-1720.

Ruiz, M. O., Chaves, L. F., Hamer, G. L., Sun, T., Brown, W. M., Walker, E. D., Haramis, L., Goldberg, T. L. & Kitron, U. D. (2010). "Local impact of temperature and precipitation on West Nile virus infection in Culex species mosquitoes in northeast Illinois, USA." *Parasites & Vectors* 3(19).

Sarrat, C., Lemonsu, A., Masson, V. & Guedalia, D. (2006). "Impact of urban heat island on regional atmospheric pollution." *Atmospheric Environment* 40(10): 1743-1758.

Scargle, J. D. (1982). "Studies in astronomical time series analysis. II-Statistical aspects of spectral analysis of unevenly spaced data." *The Astrophysical Journal* 263: 835-853.

Schott, J. R., Hook, S. J., Barsi, J. A., Markham, B. L., Miller, J., Padula, F. P. & Raqueno, N. G. (2012). "Thermal infrared radiometric calibration of the entire Landsat 4, 5, and 7 archive (1982-2010)." *Remote Sensing of Environment* 122: 41-49.

Schwarz, N., Lautenbach, S. & Seppelt, R. (2011). "Exploring indicators for quantifying surface urban heat islands of European cities with MODIS land surface temperatures." *Remote Sensing of Environment* 115(12): 3175-3186.

Seto, K. C. (2011). "Exploring the dynamics of migration to mega-delta cities in Asia and Africa: Contemporary drivers and future scenarios." *Global Environmental Change-Human and Policy Dimensions* 21: S94-S107.

Snyder, W. C., Wan, Z., Zhang, Y. & Feng, Y. Z. (1998). "Classification-based emissivity for land surface temperature measurement from space." *International Journal of Remote Sensing* 19(14): 2753-2774.

Sobrino, J. A., Jimenez-Munoz, J. C. & Paolini, L. (2004). "Land surface temperature retrieval from LANDSAT TM 5." *Remote Sensing of Environment* 90(4): 434-440.

Sobrino, J. A., Jimenez-Munoz, J. C., Soria, G., Romaguera, M., Guanter, L., Moreno, J., Plaza, A. & Martincz, P. (2008). "Land surface emissivity retrieval from different VNIR and TIR sensors." *Ieee Transactions on Geoscience and Remote Sensing* 46(2): 316-327.

Sobrino, J. A., Li, Z. L., Stoll, M. P. & Becker, F. (1996). "Multi-channel and multi-angle algorithms for estimating sea and land surface temperature with ATSR data." *International Journal of Remote Sensing* 17(11): 2089-2114.

Streutker, D. R. (2003). "Satellite-measured growth of the urban heat island of Houston, Texas." *Remote Sensing of Environment* 85(3): 282-289.

Svensson, M. K. & Eliasson, I. (2002). "Diurnal air temperatures in built-up areas in relation to urban planning." *Landscape and Urban Planning* 61(1): 37-54.

Thomson, D. J. (1995). "The Seasons, Global Temperature, and Precession." *Science* 268(5207): 59-68.

Tomlinson, C. J., Chapman, L., Thornes, J. E. & Baker, C. J. (2012). "Derivation of Birmingham's summer surface urban heat island from MODIS satellite images." *International Journal of Climatology* 32(2): 214-224.

Turner, M. G., Gardner, R. H. & O'Neill, R. V. (2001). Landscape Ecology in Theory and Practice: Pattern and Process, Springer.

Van De Kerchove, R., Lhermitte, S., Veraverbeke, S. & Goossens, R. (2013). "Spatio-temporal variability in remotely sensed land surface temperature, and its relationship with physiographic variables in the Russian Altay Mountains." *International Journal of Applied Earth Observation and Geoinformation* 20: 4-19.

Verbesselt, J., Hyndman, R., Zeileis, A. & Culvenor, D. (2010). "Phenological change detection while accounting for abrupt and gradual trends in satellite image time series." *Remote Sensing of Environment* 114(12): 2970-2980.

Voogt, J. A. & Oke, T. R. (2003). "Thermal remote sensing of urban climates." *Remote Sensing of Environment* 86(3): 370-384.

Wagenseil, H. & Samimi, C. (2006). "Assessing spatio-temporal variations in plant phenology using Fourier analysis on NDVI time series: results from a dry savannah environment in Namibia." *International Journal of Remote Sensing* 27(16): 3455-3471.

Watson, K. (1992). "Spectral Ratio Method for Measuring Emissivity." *Remote Sensing of Environment* 42(2): 113-116.

Weng, Q. & Fu, P. (2014). "Modeling annual parameters of clear-sky land surface temperature variations and evaluating the impact of cloud cover using time series of Landsat TIR data." *Remote Sensing of Environment* 140: 267-278.

Weng, Q., Liu, H. & Lu, D. (2007). "Assessing the effects of land use and land cover patterns on thermal conditions using landscape metrics in city of Indianapolis, United States." *Urban Ecosystems* 10(2): 203-219.

Weng, Q., Lu, D. S. & Schubring, J. (2004). "Estimation of land surface temperature-vegetation abundance relationship for urban heat island studies." *Remote Sensing of Environment* 89(4): 467-483.

Weng, Q., Rajasekar, U. & Hu, X. F. (2011). "Modeling Urban Heat Islands and Their Relationship With Impervious Surface and Vegetation Abundance by Using ASTER Images." *IEEE Transactions on Geoscience and Remote Sensing* 49(10): 4080-4089.

Wulder, M. A., White, J. C., Goward, S. N., Masek, J. G., Irons, J. R., Herold, M., Cohen, W. B., Loveland, T. R. & Woodcock, C. E. (2008). "Landsat continuity: Issues and opportunities for land cover monitoring." *Remote Sensing of Environment* 112(3): 955-969.

Xian, G. & Crane, M. (2006). "An analysis of urban thermal characteristics and associated land cover in Tampa Bay and Las Vegas using Landsat satellite data." *Remote Sensing of Environment* 104(2): 147-156.

Yuan, F. & Bauer, M. E. (2007). "Comparison of impervious surface area and normalized difference vegetation index as indicators of surface urban heat island effects in Landsat imagery." *Remote Sensing of Environment* 106(3): 375-386.

Zakšek, K. & Oštir, K. (2012). "Downscaling land surface temperature for urban heat island diurnal cycle analysis." *Remote Sensing of Environment* 117: 114-124.

Zhang, J. Q. & Wang, Y. P. (2008). "Study of the Relationships between the Spatial Extent of Surface Urban Heat Islands and Urban Characteristic Factors Based on Landsat ETM plus Data." *Sensors* 8(11): 7453-7468.

Zhou, Y. Y., Weng, Q. H., Gurney, K. R., Shuai, Y. M. & Hu, X. F. (2012). "Estimation of the relationship between remotely sensed anthropogenic heat discharge and building energy use." *ISPRS Journal of Photogrammetry and Remote Sensing* 67: 65-72.

Zhu, Z., Woodcock, C. (2014). "Continuous change detection and classification of land cover using all available Landsat data." *Remote Sensing of Environment* 144: 152-171.